Nanoscale

ROYAL SOCIETY OF CHEMISTRY

MINIREVIEW

View Article Online
View Journal | View Issue

Check for updates

Cite this: *Nanoscale*, 2023, **15**, 13202

Nanoparticles with transformable physicochemical properties for overcoming biological barriers

Qianqian Lu,[a] Hongyue Yu,[a] Tiancong Zhao,*[a] Guanjia Zhu *[b] and Xiaomin Li *[a]

In recent years, tremendous progress has been made in the development of nanomedicines for advanced therapeutics, yet their unsatisfactory targeting ability hinders the further application of nanomedicines. Nanomaterials undergo a series of processes, from intravenous injection to precise delivery at target sites. Each process faces different or even contradictory requirements for nanoparticles to pass through biological barriers. To overcome biological barriers, researchers have been developing nanomedicines with transformable physicochemical properties in recent years. Physicochemical transformability enables nanomedicines to responsively switch their physicochemical properties, including size, shape, surface charge, *etc.*, thus enabling them to cross a series of biological barriers and achieve maximum delivery efficiency. In this review, we summarize recent developments in nanomedicines with transformable physicochemical properties. First, the biological dilemmas faced by nanomedicines are analyzed. Furthermore, the design and synthesis of nanomaterials with transformable physicochemical properties in terms of size, charge, and shape are summarized. Other switchable physicochemical parameters such as mobility, roughness and mechanical properties, which have been sought after most recently, are also discussed. Finally, the prospects and challenges for nanomedicines with transformable physicochemical properties are highlighted.

Received 22nd March 2023,
Accepted 9th July 2023

DOI: 10.1039/d3nr01332d

rsc.li/nanoscale

Published on 14 July 2023. Downloaded on 7/11/2024 11:04:51 PM.

1 Introduction

Nanomedicines provide a new approach for the diagnosis and treatment of diseases.[1] With the rapid development of nanobiotechnology, nanomedicines are expected to provide new treatment strategies and enhance therapeutic efficacy.[2] Several chemotherapeutic nanomedicines, with the advantages of long circulation time in the blood, efficient site-specific accumulation and relatively few side effects, have been approved for clinical therapy.[3] In recent years, nanomedicines

[a]*Department of Chemistry, Laboratory of Advanced Materials, Shanghai Key Laboratory of Molecular Catalysis and Innovative Materials, State Key Laboratory of Molecular Engineering of Polymers, Collaborative Innovation Center of Chemistry for Energy Materials (2011-iChEM), Fudan University, Shanghai 200433, P. R. China. E-mail: zhao_tc@fudan.edu.cn, lixm@fudan.edu.cn*
[b]*Institute of Nanochemistry and Nanobiology, Shanghai University, Shanghai 200444, P. R. China. E-mail: zhuguanjia@shu.edu.cn*

Qianqian Lu

Qianqian Lu was born in Jingzhou, Hubei, in June, 1999. She received her B.E. degree from Hubei University in 2021. She is working for her master's degree under the guidance of Prof. Xiaomin Li at Fudan University. Her current research mainly focuses on designing and developing a drug delivery system with transformable physicochemical properties for tumor therapy.

Hongyue Yu

Hongyue Yu was born in Liaoning, China, in 1997. She received her B.E. degree from the Dalian University of Technology in 2019. Since then, she has been studying as a Ph.D. student at Fudan University in China under the supervision of Prof. Xiaomin Li. Her current research interests focus on the synthesis of silica/metal compound mesoporous materials and their applications in the biomedical field.

This journal is © The Royal Society of Chemistry 2023

Published on 14 July 2023. Downloaded on 7/11/2024 11:04:51 PM.

have shown excellent application and development prospects for drug delivery and improving treatment efficacy.[4]

However, current nanomedicines have failed to improve overall treatment efficiencies due to a series of problems. Among them, the unsatisfactory delivery efficiency of nanoparticles to lesions is a major scientific problem that needs to be solved urgently due to multiple biological barriers.[5] Generally, an intravenously administered nanomedicine must go through a cascade of five steps before reaching the target tumor cells: intravenous injection into the blood circulation, accumulation at the tumor site through infiltration and retention effects, penetration into the tumor tissue, endocytosis and intracellular drug release.[6] In each process, different biological barriers are faced, such as the vascular barrier, matrix barrier, and cell membrane-specific selection, which more or less hinder the *in vivo* delivery of nanomedicines and thus lead to low drug efficacy.[7] Nanoparticles' physicochemical properties, including shape, charge, size and so on, significantly affect their interactions with biological barriers.[8–10] However, scientists find that the required physicochemical properties are different and even opposing in different steps.[11] Therefore, to overcome the abovementioned dilemmas, scientists have proposed physicochemical transformable nanomaterials for enhanced biological applications.[12–14]

Physicochemical transformable nanomaterials are a relatively new research field. Although there are many reviews on the design of nanomaterials to overcome biological barriers to drug delivery, they only focus on how one of the physicochemical properties affects nano-biological interactions.[15–17] Herein, we present a review of the design, synthesis, and application of nanomaterials with transformable physicochemical properties. Along this line, this review analyzes a range of smart nanoparticles with transformable physicochemical properties (size, shape, charge, stiffness, *etc*.). It summarizes specifically how each material is designed and how it "responds" to internal/external stimuli. Finally, future research to develop high performances and the clinical translation of nanomedicines is also discussed.

2 Demands during nanoparticle delivery

2.1 Long circulation time

Following intravenous injection, nanoparticles are carried through the body by blood vessels. The longer nanoparticles circulate in the bloodstream, the more they are accumulated in tumor tissue.[18] During the journey in the blood, the main factors affecting the nanoparticles' circulation time include protein corona adsorption, phagocytosis, and physical filtration, which may lead to the clearance of nanoparticles and reduced delivery efficiency.[19,20] The physicochemical properties can influence the interaction of these biological barriers with nanomaterials.[21] For example, clearance of the mononuclear phagocyte system (MPS) exhibits size-dependent behavior, and nanomaterials with sizes smaller than 20 nm are rapidly cleared.[22] Macrophage phagocytosis also quickly clears exceptionally large particles (more than a few microns). So, the range from a hundred nanometers to the micron level is the most appropriate size.[23] In terms of surface charge, most proteins in the blood are negatively charged, and so are the cell membranes. Therefore, nanomaterials with a negative surface charge are more likely to evade phagocytosis by macrophages, while positively charged nanoparticles have a higher tendency to be cleared by macrophages due to electrostatic attraction.[24,25] Also, when it comes to the shape of nanoparticles, researchers have been reporting diverse results. Nanospheres, nanorods, nanosheets, and fibers all have their unique nano–bio interactions and significantly different *in vivo* behaviors.[26]

2.2 Lesion accumulation

After being carried to the target lesion, nanomedicines need to accumulate at the site so as to perform their therapeutic effects. In the case of solid tumors, nanomedicines accumulate passively in tumor tissue through enhanced permeability and retention (EPR) effects by exploiting the permeable vascular systems and defective lymphatic vessels.[27] Depending on the rationale of the EPR effect, since nanomedicines have to cross

Tiancong Zhao

Dr Tiancong Zhao received his Ph.D. from Dongyuan Zhao/Xiaomin Li's group at Fudan University and is currently a postdoctoral researcher in the same group. His research is centered on the design, synthesis and application of novel porous nanomaterials.

Guanjia Zhu

Dr Guanjia Zhu received her Ph.D. in 2020 from Donghua University. And in the same year, she joined the School of Environmental and Chemical Engineering at Shanghai University. Her current research interests focus on silicon-based functional materials.

Published on 14 July 2023. Downloaded on 7/11/2024 11:04:51 PM.

the breakage of blood vessels to enter the tumor, the size of nanomedicines is most critical in this process, and the area of blood vessel breakage is usually several hundred nanometers.[28] Considering the circulation requirement (that nanomedicines smaller than 20 nm will be quickly cleared out), 100–200 nm is generally considered the optimal particle size for the EPR effect. Therefore, previous works have mainly used nanomedicines in this size range. In addition, some research teams have recently proposed a new mechanism for the active penetration of nanomedicines in tissues, mainly utilizing the principle of the mutual attraction of positive and negative charges. For instance, Shen's team developed an active transport liposome that could actively cross the biological barrier with responsive cationization-triggered cytosolic transport for targeted enrichment and deep penetration drug delivery in hepatocellular and pancreatic cancers, with promising therapeutic effects in a variety of solid tumor models of hepatocellular and pancreatic cancers. Hence, the surface charge of nanomedicines is also significant for their enrichment in tumors.[29,30]

2.3 Deep penetration

Usually, lesions are of a specific range and depth. For example, tumors are solid entities that limit the nanomedicines' intratumoral penetration and distribution. A dense extracellular matrix, tightly packed tumor cells, and high interstitial fluid pressure accumulate to form solid stresses.[31–33] Poorly structured and unevenly distributed blood vessels lead to the nanomedicines' uneven spatial distribution in tumors. These together form an abnormal tumor microenvironment (TME) and act as pathological barriers that prevent nanomedicines from entering cancer cells.[18,34] To make matters worse, the size of nanomedicines at the nanoscale severely limits their extravasation and penetration from the vasculature into the tumor tissue. Therefore, successful nanomedicines need to extravasate and deeply penetrate efficiently. Numerous studies have shown that nanoparticles with particles smaller than 20 nm are more suitable for penetration into deep tumor layers.[16] This diameter then contradicts the previously described size to facilitate cyclic enrichment.

Xiaomin Li

Prof. Xiaomin Li received his Ph.D. in 2014 from Fudan University followed by 2 years postdoctoral experience at Fudan University and Griffith University. He joined the Chemistry Department of Fudan University in 2016. His current research interests include the development of multifunctional nanostructured materials and nanotechnology for applications in bioimaging, nanomedicine, analysis, and drug delivery.

2.4 Cellular internalization

In the process of targeted drug delivery, it is malignant cells that ultimately need to be eliminated. Therefore, after a long process of blood circulation, tumor accumulation, and extracellular matrix penetration, nanomedicines need to be effectively internalized by cancer cells.[27] The cell membrane is a phospholipid bilayer inlaid with many proteins that separate the inside and outside of the cell and dominate the exchange of substances between the cell and the outside environment. Hence, the cell membrane is a natural barrier to the nanomedicine's cellular internalization, which makes the interaction between nanomaterials and cell membranes crucial.[35] Research has shown that the size, shape, and charge of nanoparticles all affect the interaction between nanoparticles and cell membranes. Particles with different diameters have different mechanisms through which they are taken up by cells.[36] Different shapes also perturb cell membranes in various forms, altering the take up rate. For example, it is generally believed that cells take up rod-shaped particles faster than spherical particles because a larger aspect ratio can perturb more cell membrane bending.[37,38] Surface roughness also contributes to enhanced cellular take up.[39] However, if nanoparticles are easily taken up by the tumor cell, they would inevitably also have a strong tendency to enhanced take up by a macrophage, leading to quick elimination from the blood and a low targeting efficiency. Therefore, new approaches are required to solve the problem.

From the requirements above, the conditions at different stages are completely different, complex and variable, even contradictory. However, conventionally used nanoparticles have inflexible properties and are unable to meet all the requirements at the same time. Therefore, in order to overcome the multiple physiological barriers faced in the treatment process, nanoparticles need to achieve specific transformations in physicochemical properties. In recent years, many researchers have taken full advantage of existing paradoxes to design a range of intelligent nanoparticles with tunable physicochemical properties, including switching ability in terms of particle size, particle shape, surface charge, roughness, mechanical properties, and so on, as shown in Fig. 1. In the following sections, we summarize and discuss recent advances in the development of transformable nanoparticles based on various physicochemical properties.

3 Stimulus-responsive nanoparticles with transformable physicochemical properties

3.1 Size transformation

As one of the most important characteristics of nanoparticles, size greatly influences the efficiency of the targeted delivery of nanoparticles in many ways.[40] Nanoparticles with a particle size of 100–200 nm have a good long circulation and accumulation effect, but they do not favour diffusion into solid

 This journal is © The Royal Society of Chemistry 2023

Published on 14 July 2023. Downloaded on 7/11/2024 11:04:51 PM.

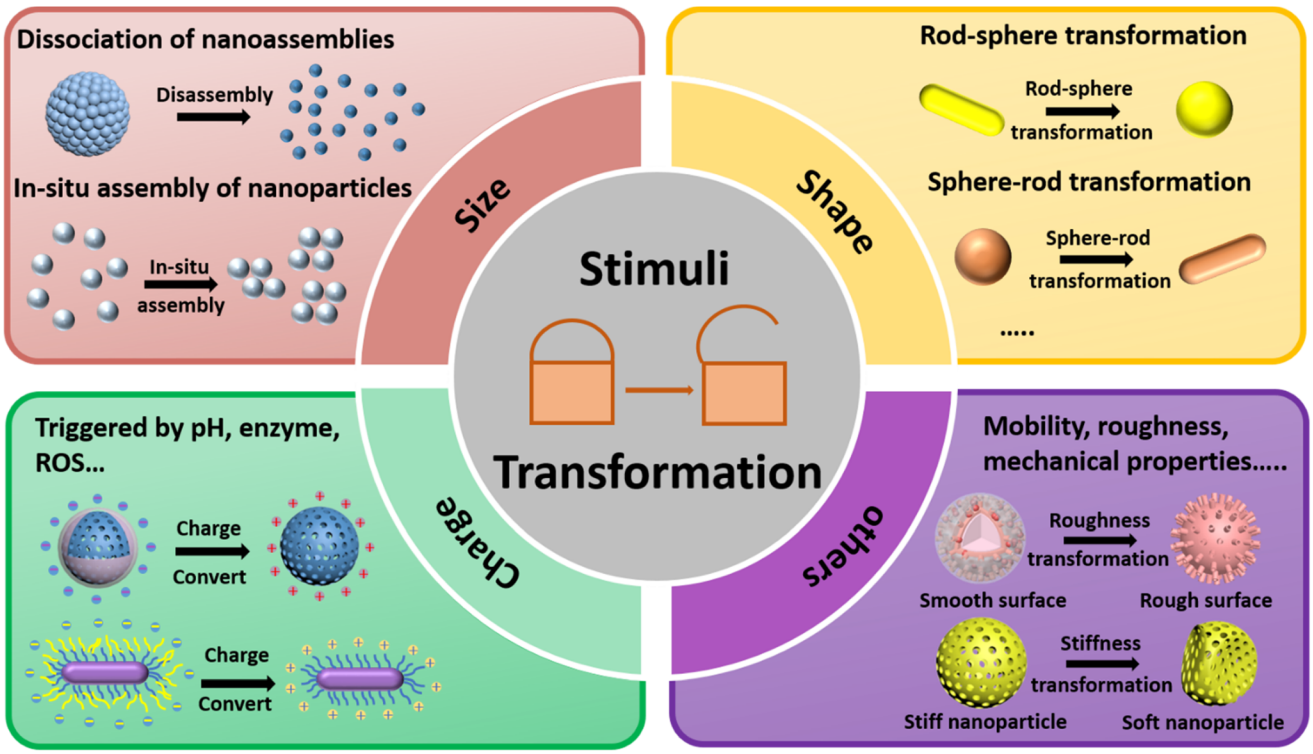

Fig. 1 A brief illustration of intelligent transformable nanomaterials based on various physicochemical properties.

tumors, and most nanoparticles spill out of the tumor vasculature.[41] Nanoparticles with particle sizes smaller than 20 nm are more likely to penetrate deeper into the tumor, but they are rapidly cleared out from the blood and cannot achieve high tumor accumulation.[6] Therefore, nanoparticles should first have a relatively large diameter for long blood circulation and EPR (100–200 nm) to accumulate and penetrate tumors with high efficiency. Upon accumulating at the tumor, the size should shift to small sizes (<20 nm) for efficient tumor penetration. There are also other applications, such as imaging, where we need nanoparticles to remain in the appropriate location for a long time. In this case, we want the nanoparticles to penetrate the organ with a small size and transform into a larger size after penetration to avoid metabolism.[42] For optimal performance, size-switchable nanoparticles have an extraordinary talent. Compared to uniquely sized nanoparticles, size-switchable nanoparticles can achieve better penetration and retention by simply switching their size at a suitable time.[43] This section summarizes some of the developed methods for preparing size-switchable nanoparticles.

3.1.1 Dissociation of nanoassemblies. The size reduction strategy is essentially a process of responsive disassembly of "linked" large-size materials at a specific target lesion. The size-reducible nanoparticles not only retain a small size for enhanced permeability, but also contribute to many other properties, such as secondary distribution,[44] drug release,[45] *etc*. By now, plenty of nanoparticles have been investigated based on the endogenous acidic pH,[46–48] overexpressed enzymes,[49,50] redox conditions and exogenous physicochemical stimuli;[51–53] these are discussed in the following.

As it is known to all, many lesions, such as the tumor microenvironment and lysosomes, are more acidic compared to other tissues. Many efforts focus on nanoscale drug delivery systems that utilize the pH gradient of the disease microenvironment as a trigger for initiating conformational changes, leading to drug release. In recent years, polymeric materials doped with maleic acid amides (MAA) have been found to have pH-responsive characteristics.[54] MAA-based materials are usually synthesized by reacting the segment's amino groups with maleic acid (MA) or its derivatives.[55,56] Under acidic conditions, the carboxyl group attacks the neighboring carbonyl group to form a succinic anhydride intermediate, contributing to the amide bond's breakage. Based on this principle, MAA-based nanomedicines can be easily degraded into small particles at the tumor site.[46,57] For instance, Li *et al.* fixed cisplatin-loaded polyamidoamine dendrimers (PAMAM/Pt) to the end of a block-copolymer through amino–carboxyl coupling. The block-copolymer is made up of polycaprolactone (PCL) and 2-propionic acid-3-methylmaleic anhydride (MA derivative, CDM). Through the assembly of polymers, the small-sized dendrimers (~5 nm) are assembled into a large nanoparticle with a diameter of ~100 nm. Upon reaching the tumor site, the acidity triggers breakages between the amino group of PAMAM and the carboxyl residues of CDM and releases the small-sized PAMAM/Pt dendrimers. The size shrinks from 100 nm to 5 nm under the acidic tumor extracellular microenvironment (~pH 6.5) to enable better penetration into deep tumor tissue

Published on 14 July 2023. Downloaded on 7/11/2024 11:04:51 PM.

(Fig. 2a).[46] Similar works have also been done in other systems using maleic acid amide nanomaterials.[45]

The Schiff base is another widely used pH-sensitive chemical group characterized by forming a double bond between carbon and nitrogen atoms (–CN–); this bond is unstable at acidic pH and easily broken through hydrolysis.[58] Guo *et al.* designed a nanomaterial that could be induced to change size by an acid and had a good tumor penetration ability. Small dendritic poly-L-lysine (DGL) nanoparticles with a diameter of ~10 nm were first synthesized. Then an aldehyde group

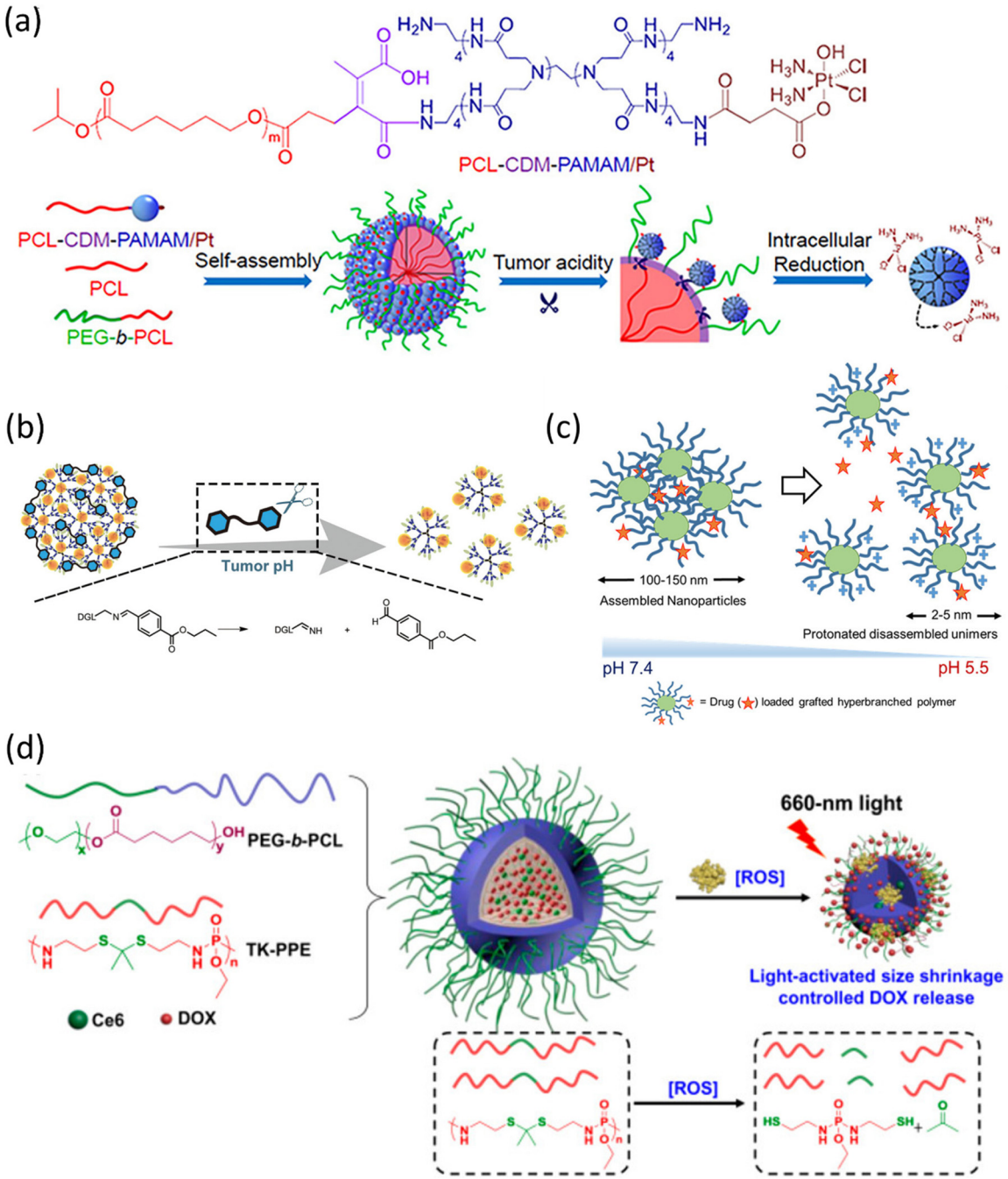

Fig. 2 (a) Chemical structure of PCL-CMD-PAMAM/Pt, self-assembly and structural change to iCluster/Pt in response to tumor acidity and intracellular reducing environment.[46] Reproduced from ref. 46 with permission from the National Academy of Sciences, copyright 2016. (b) Schematic illustration showing the disintegration of large NPs into small particles at tumor acidic pH.[47] Reproduced from ref. 47 with permission from Wiley-VCH GmbH, copyright 2019. (c) Mechanism of pH-induced assembly and disassembly of the nanoparticles mediated through protonation/deprotonation of grafted segments.[48] Reproduced from ref. 48 with permission from the American Chemical Society, copyright 2019. (d) Formation and mechanism of light-activated reducible TK-PPE@NPce6/DOX nanoparticle.[51] Reproduced from ref. 51 with permission from the American Chemical Society, copyright 2017.

 This journal is © The Royal Society of Chemistry 2023

Published on 14 July 2023. Downloaded on 7/11/2024 11:04:51 PM.

containing a linker (1,6-bis(4-formylbenzoyloxy)hexane) is used to crosslink the DGLs to form large-sized spherical nanomaterials (~123 nm). The linker forms Schiff base bonds with DGLs in a neutral environment. In contrast, in an acidic tumor environment, the bonds are hydrolyzed and broken, leading to the disassembly of large particles and the release of small DGLs, resulting in a switch in size from 123 nm to 10 nm. With this switch, both enhanced penetration into *in vitro* 3D triple-negative breast cancer spheroids and *in vivo* tumor tissues (Fig. 2b) are shown.[47]

Polymers functionalized with amino groups are usually unprotonated at neutral pH and exhibit hydrophobicity. Hydrophobic polymers tend to aggregate into large-sized particles.[59] However, the amino groups become hydrophilic when protonated under acidic pH conditions, which disintegrates the large particles and leads to size switching.[60] Ray *et al.* designed small poly(carbonate) nanoparticles with a diameter of ~5 nm, and the surface of the nanoparticles was modified with amino groups containing polymer grafts. In a neutral environment, the unprotonated hydrophobic grafts direct the nanoparticles to assemble into a large-sized aggregate (~150 nm). Upon reaching the tumor acidic microenvironment, the amine groups undergo protonation, making the polymers hydrophilic and resulting in the disassembly of the nanoparticles and size switching from 150–190 nm to 3–5 nm (Fig. 2c).[48] Collectively, a reduction in size takes effect near localized disease targets in response to microenvironmental triggers. Wang and colleagues have also similarly synthesized amino polymer nanoparticles with acid response switches; this increases the cellular take up of the drug.[61]

Zhao *et al.* also reported the fabrication of ~200 nm nanocapsules assembled from ~20 nm upconversion nanoparticles (UCNPs) with polymers containing azo groups. The suitable size enables the nanocapsules to achieve high tumor accumulation. Upon NIR irradiation, UCNPs transfer NIR light to UV/vis light, which activates the *trans*/*cis* switching of azo groups in the polymer. This conformation switch leads to breakage of the nanocapsule, achieving a size switch from ~200 nm to ~20 nm, and thus, rapid elimination from the tumor within one hour and release of the loaded drugs for chemotherapy.[53]

Since the GSH level is critical in the tumor tissue and cytoplasm, its responsiveness is also evident from size reduction strategies. The specific process is to introduce disulfide bonds susceptible to GSH cleavage for responsive redox biomaterials. For instance, Ma *et al.* utilized cystamine, a small molecule with disulfide bonds and amino ends, to assemble tannic acid into large-size nano-assemblies (~170 nm). When triggered by GSH, the disulfide bonds break and lead to the degradation of the nano-assemblies into small-sized nanoparticles with a diameter of ~20 nm. This size transformation promises to overcome rapid renal clearance and hampered deep tumor penetration.[62] Guo and coworkers have done similar work to design a GSH response system to achieve nanoparticle size switching from 150 nm to 7.2 nm, enabling efficient therapy and imaging of tumors for enhanced tumor theranostics.[63]

Abnormal intracellular reactive oxygen species (ROS) levels could also be used to develop stimuli-responsive nanocarriers. It is well known that ROS levels in cancer cells (~10 μM) are higher compared to normal tissues (~10 nM).[51,64] Nano-assemblies of photosensitizer–drug complex nanomaterials developed based on ROS-responsive interactions provide a versatile nano-platform for deep tumor penetration and synergistic photochemotherapy.[65] Cao and colleagues synthesized ROS-sensitive polymeric nanocarrier-based TK-PPE@$NP_{Ce6/DOX}$ for nanocarrier drug delivery. Chlorin e6 (Ce6) and Adriamycin (DOX) are encapsulated in ROS-sensitive poly(thioketal phosphoester) (TK-PPE) polymer nanoparticles with a diameter of 154 nm. Under 660 nm red light excitation, the ROS generated by encapsulated Ce6 was able to *in situ* cleave the condensed thioketal chemical bond in the TK junction, leading to rapid degradation of the nano-assembly core and a size reduction from 154 ± 4 nm to 72 ± 3 nm (Fig. 2d), and such size transformation affected further triggered rapid DOX release.[51] Other work has used similar designs for functional groups other than the thioketal phosphoester that respond to ROS switches, including polypropylene sulfide,[66] phenylboronic ester,[67] thioketal and so on.[68]

Several inorganic nanomaterials have been developed to show a pH-responsive reduction, such as manganese (Mn)-containing nanomaterials, calcium (Ca)-containing nanocarriers, and metal–organic frameworks.[69–71] When small-sized nanoparticles are loaded within large-sized inorganic materials, the reduction of carriers releases the small "cargos", achieving a size switch. Wang *et al.* prepared amorphous calcium carbonate nanoparticles (ACC) pre-loaded with DOX. When approaching the tumor area, due to the acid instability of the ACC, it will dissolve and release DOX in the form of small-sized nano-assemblies. The reduction of nanocarrier size enables better drug permeability into the solid tumor.[72] In a similar fashion, Sun *et al.* prepared ZIF-8 based nanomedicine. The size-shifting behavior is the same as that of ACC (Fig. 3a).[73] In addition to the above inorganic carriers, silica nanomaterials are often used in similar designs. For example, Kim *et al.* developed a mesoporous silica nanoparticle (MSN) as a carrier in which the large pore size enabled the loading of many gold nanoparticles (AuNPs). The AuNPs were programmed by DNA hybridization to reduce the leakage of AuNPs in the blood circulation; when reaching the tumor's acidic environment, the DNA dissociates in response to pH and releases small gold particles for deep-penetrating 3D cancer therapy.[74]

Many tumor-specific enzymes were found to be overproduced, such as matrix metalloproteinase-2 (MMP-2), hyaluronidase (HAase) and fibroblast activation protein-α (FAP-α).[75,76] The enzyme has a high catalytic activity for some substances while being highly selective and does not affect others. In this way, the small-sized nanoparticles can be encapsulated or loaded in a carrier that the enzyme can degrade. After reaching the tumor site, the large-sized nanocarrier degrades and releases small-sized nanoparticles.[77] Recently, specific enzyme-sensitive tailor-made peptides were utilized to construct enzyme-degradable nanocarriers. For instance, size-

Published on 14 July 2023. Downloaded on 7/11/2024 11:04:51 PM.

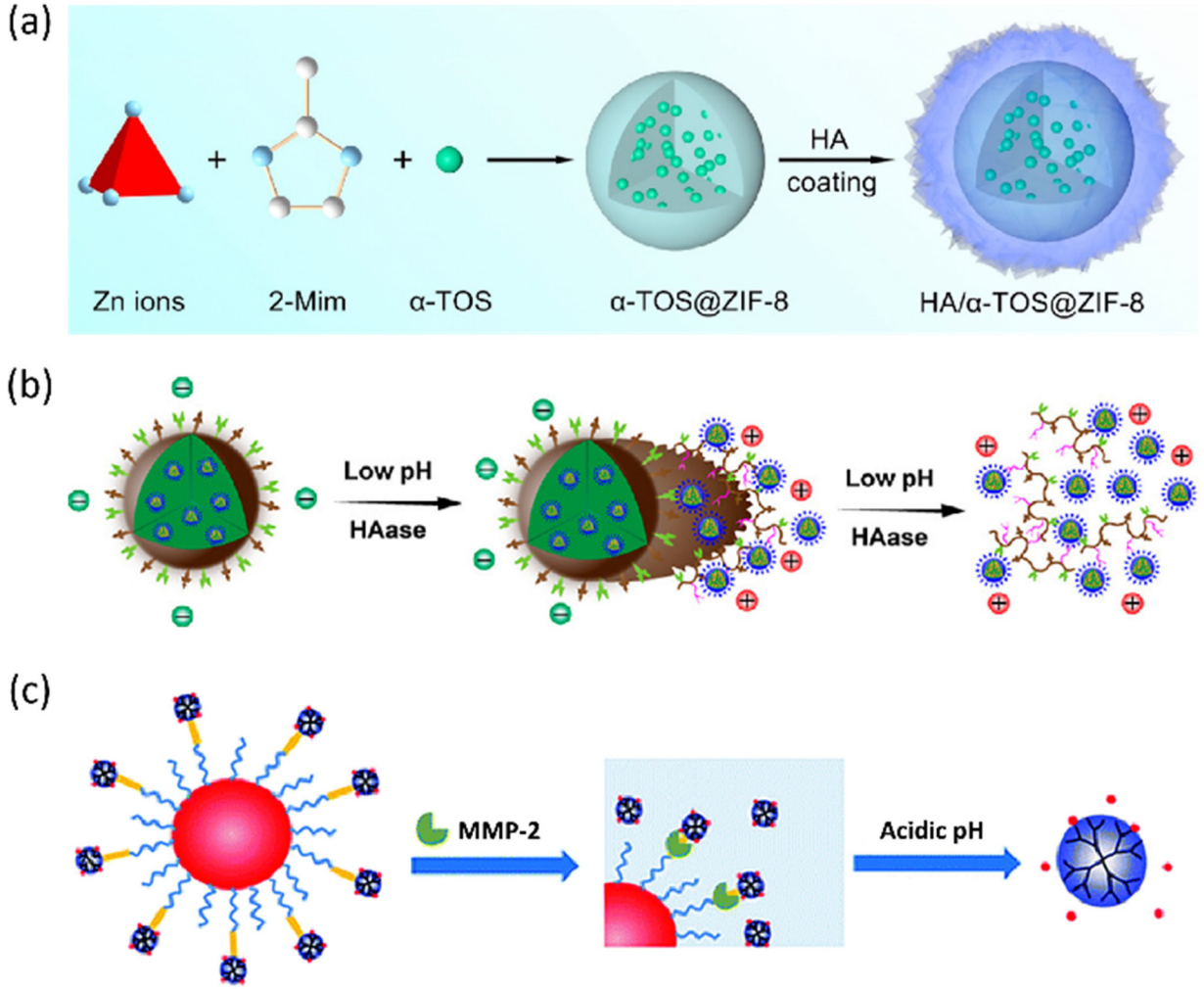

Fig. 3 (a) Schematic illustration of the formation of the HA/α-TOS@ZIF-8 nano-platform.[73] Reproduced from ref. 73 with permission from Elsevier B.V., copyright 2019. (b) Schematic illustration of the transformation of hICP NPs triggered by HAase and acidic pH.[50] Reproduced from ref. 50 with permission from the American Chemical Society, copyright 2020. (c) Schematic illustration showing the size change in response to MMP-2 in the TME and drug release in response to intracellular acidic pH.[49] Reproduced from ref. 49 with permission from the Royal Society of Chemistry, copyright 2018.

reducible nanocarriers based on the self-assembly of acetyl hyaluronate (HA) were reported by Zhao and colleagues. They encapsulated small amphiphilic hexadecapeptide derivative nanoparticles (130 nm) into dopamine-modified hyaluronate nanocarriers. When overexpressed hyaluronidase in the TEM dissociated the hyaluronate carriers, the small hexadecapeptide nanoparticles were released, achieving a size switching from 130 nm to 30 nm (Fig. 3b). This process is also accompanied by a shift in surface charge, from the dopamine-modified negative surface to positively charged peptides, further enhancing tumor penetration.[50] Similarly, Cun *et al.* constructed an MMP-sensitive responsive nano-platform. Small nanoparticles (~30 nm) can be released when the MMPase-sensitive peptide fragments in larger nanoparticles (~100 nm) are cleaved. This size-adjustable nano-platform provides a multifunctional strategy for TEM modulation and tumor penetration (Fig. 3c).[49]

3.1.2 *In situ* assembly of nanoparticles. As contradictory behavior to the varied sizes described above, small-sized nanoparticles tend to have good penetration. They are cleared rapidly, while nanoparticles with large sizes have enhanced retention time but cannot penetrate deeply into tumors. Researchers proposed a self-assembly strategy to enhance the accumulation and penetration of nanoparticles in the meantime, which could be used for enhanced cellular take up, antimetastasis, and tumor diagnosis.[78,79] In some instances, small-sized nanoparticles are first used for deep penetration and responsively assembled into large aggregates in the tumor to enhance the retention capability. The stimulations can be classified into several types due to tumor heterogeneity, such as host–guest interactions,[79] a slightly acidic microenvironment,[80,81] and specific up-regulation of enzymes.[82,83] In addition, most current research hotspots focus on applying some external stimulus, such as light, which

 This journal is © The Royal Society of Chemistry 2023

Published on 14 July 2023. Downloaded on 7/11/2024 11:04:51 PM.

is often used to trigger the *in situ* assembly of nanoparticles.[84,85]

Recently, tremendous efforts were devoted to improving the tumor accumulation of nanoprobes by host–guest interactions. For example, Professor Fan Zhang's team designed a probe based on the host–guest interactions between azobenzene-modified rare-Earth upconversion nanoparticles (UCNP@Azo) and β-cyclodextrin-modified NIR-II rare-Earth downconversion nanoprobes (DCNP@β-CD) (Fig. 4a). Small-sized UCNP@Azo and DCNP@β-CD are injected separately to attain deep tumor penetration, and locking between Azo and β-CD enables the assembly of the two to achieve a long retention time in the tumor. This method enables contrast agent enrichment in tumors by approximately 4-fold, significantly enhancing the imaging performance (Fig. 4b).[42] For instance, Wang *et al.* synthesized NIR-II down-conversion rare Earth nanoparticles (DCNPs) with a diameter of ~7.7 nm. By modifying paired DNA (L1/L2) and targeting protein (FSH β) on their surfaces, respectively, DCNPs self-assemble and aggregate at tumor tissues by exploiting the paired nature of DNA, achieving long-term stable labelling of the probes within the tumor and significantly improving the signal-to-noise ratio of optical imaging (Fig. 4c).[86]

There are many specific upregulated enzymes in tumor tissues, such as matrix metalloproteinase (MMP), legumain, hyaluronidase (HAase), gelatinase,[87] furin,[88] proteases,[89] *etc*. Bellat *et al.* reported functional peptide nanofibers to achieve *in situ* assembly triggered by tumor-associated proteases for the treatment of breast cancer. They reported a peptide-based nanofiber precursor (NFP) composed of multiple β-sheet peptides (mPEG2000-KLDLKLDLKLDL-$CONH_2$). Each peptide comprises alternating hydrophobic and hydrophilic residues conjugated to a methoxypolyethylene glycol (mPEG) chain. mPEG prevents interfibril aggregation. Immediately after the cleavage of hydrophilic mPEG by proteases (*via* the N-terminal lysine of the peptide construct), NFP became extremely hydrophobic. To improve solubility, multiple nanofibers are assembled into 10× larger inter-fibril networks, thus showing lower tumoral take up and a prolonged retention time (Fig. 4d).[89]

Different from enzyme-induced *in situ* assembly, pH-triggered reactions possess the advantages of a quick response and ultrasensitivity. pH-responsive molecules are usually zwitterionic compounds, such as hydrolysis-susceptible citraconic amide,[81,90] 11-mercaptoundecanoic acid, and (10-mercaptodecyl)trimethylammonium bromide.[91] For example, Hu *et al.* recently designed a nanomaterial that achieved a size shift from small to large in response to a slightly acidic microenvironment for the treatment of bacterial infection. Originally, AuNPs were readily prepared by surface modification with pH-responsive mixed charge zwitterionic self-assembled monolayers consisting of weak electrolytic 11-mercaptoundecanoic acid and strong electrolytic (10-mercaptodecyl)trimethylammonium bromide. The mixed charge zwitterion-modified AuNPs showed a fast pH-responsive transition from negative charge to positive charge, which enabled the AuNPs to disperse well in healthy tissues (pH ~7.4) while quickly presenting strong adherence to negatively charged bacteria surfaces in MRSA biofilm (pH ~5.5). Simultaneous AuNP self-assembly within the MRSA biofilm enhanced the photothermal ablation of MRSA biofilm under NIR light irradiation (Fig. 4e).[92]

Light-induced strategies show great advantages for non-invasiveness, remote manipulation, and ease of operation. In the self-assembly strategies, light-responsive polymers are supplied with photoactive groups such as spiro-benzopyran, triphenylmethane, azobenzene, or cinnamenyl, which can undergo reversible structural switches under UV-vis light.[93,94] However, the application of this strategy is limited to experiments at the cellular level due to the weak penetration ability and autofluorescence interference of UV-vis and blue light. Upconversion nanoparticles (UCNPs), usually containing lanthanide ions, are able to convert long-wavelength near-infrared (NIR) light with greatly improved tissue penetration into short-wavelength light through a multiphoton absorption/single-photon emission process.[95] Due to their unique optical properties, UCNPs have been developed for more applications, such as biomedical sensing, imaging and therapies. Recently, Xu *et al.* designed a multi-tasking UCNP for NIR-triggered photodynamic therapy combined with checkpoint blockade for immunotherapy of colorectal cancer.[96] Therefore, the further application of light-induced assembly *in vivo* can be achieved with excellent prospects by utilizing UCNPs as the carrier.

3.2 Shape transformation

In addition to the impacts of particle size on the delivery efficacy of nanomedicines, the shape of the nanostructures has also been found to impose significant effects on circulation, enrichment and metabolism of nanoparticles. Some typical shapes of nanomedicines include nanospheres, nanorods/fibers, nanosheets, and so on. As it is rather difficult to prepare a series of nanomaterials only varying in shape (not interfering with other physicochemical properties), studies on the impact of shape on nano–bio interactions are not as unequivocal as those on size. For example, some have observed that long fibers circulate longer in the blood compared to nanospheres and nanorods.[26] Yet others have reported that spherical nanoparticles have prolonged blood circulation; at the same time, nanorods/nanofibers are more likely to penetrate into the tumor further and kill tumor cells *via* physically wrapping around the cell.[10]

Regardless of these studies, one thing is for sure. Suppose a nanomaterial with one shape can avoid being phagocytosed by macrophages for longer blood circulation, there will be difficulties in internalizing it in tumor cells for better drug delivery. Therefore, selecting a specific shape that meets all requirements is impossible. Hence, nanoparticles with transformable shapes need to be designed to maximize the benefits of different shapes. This section summarizes some of the strategies used to prepare shape-transformable nanoparticles.

Published on 14 July 2023. Downloaded on 7/11/2024 11:04:51 PM.

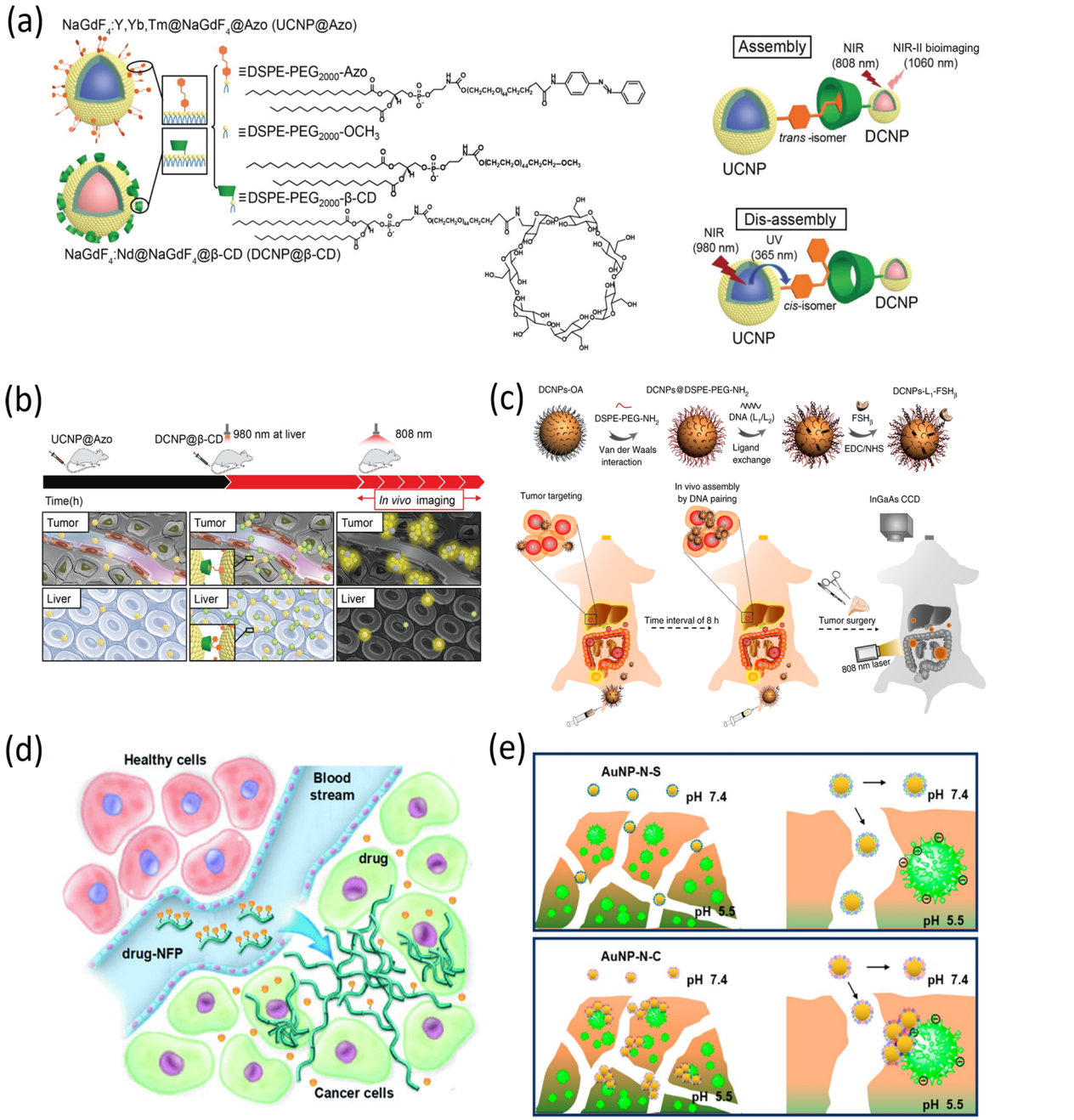

Fig. 4 (a) Preparation of azobenzene (Azo) modified $NaGdF_4$:10%Y,25%Yb,0.5%Tm@$NaGdF_4$ (UCNP@Azo) and β-CD modified $NaGdF_4$:5% Nd@$NaGdF_4$ (DCNP@β-CD).[42] Reproduced from ref. 42 with permission from Wiley-VCH GmbH, copyright 2018. (b) *In vivo* assembly of UCNP@Azo and DCNP@β-CD with improved tumor targeting.[42] Reproduced from ref. 42 with permission from Wiley-VCH GmbH, copyright 2018. (c) Schematic illustration of the stepwise preparation of DNA and FSHβ modified DCNPs (DCNPs-L1-FSHβ) and *in vivo* assembly of DCNPs-L1-FSHβ (first injection) and DCNPs-L2-FSHβ (second injection) with improved tumor targeting and rapid hepatic and renal clearance after two-stage in sequence injections.[86] Reproduced from ref. 86 with permission from Springer Nature, copyright 2018. (d) NFP has a high aspect ratio that promotes its take up by solid tumors. Multiple NFPs can penetrate tumor tissue and subsequently transform into larger interfibril networks *via in situ* activation by tumor-associated proteases, thus minimizing lymphatic clearance.[89] Reproduced from ref. 89 with permission from Wiley-VCH GmbH, copyright 2018. (e) AuNP-N–S, with negatively charged surfaces, dispersed stably in MRSA biofilm and healthy tissues but with no bactericidal effect under NIR light irradiation; AuNP-N–C, with positively charged surfaces in acidic MRSA biofilm (pH ~5.5), effectively adhered to bacteria and rapidly aggregated in MRSA biofilm, exhibiting great bactericidal effect under NIR light irradiation without damage to surrounding healthy tissues (pH ~7.4).[92] Reproduced from ref. 92 with permission from the American Chemical Society, copyright 2017.

This journal is © The Royal Society of Chemistry 2023

Published on 14 July 2023. Downloaded on 7/11/2024 11:04:51 PM.

3.2.1 Rod–sphere transformation. Rod shaped nanomaterials have a high aspect ratio, and some researchers have reported that this hinders cellular take up and tumor penetration.[97] Therefore, researchers have been working on the stimuli-responsive rod–sphere transformation of nanomaterials. Nanomaterials containing groups such as amino acids, dimethyl maleic amide, and ketals respond well to an acidic environment.[98,99] For example, in the case of amino acids, the presence of various positive and negative charges and hydrophobic/hydrophilic groups enables the self-assembly of amino acid molecules into nanostructures. In an acidic environment, specific functional groups become protonated, thereby altering the properties and assembly performance of amino acids. As a result, these nanomaterials may become unstable or undergo swelling, leading to a shape transformation. For instance, Li *et al.* constructed pH-sensitive peptide assemblies that changed shape from rod-like nanofibers to spherical morphology for enhanced drug delivery and photodynamic therapy. The team first constructed a pentapeptide assembly with a rod-like fiber shape, in which the 4-aminoproline amide bond in the material could effectively change the peptide interaction interface and thus modulate the peptide nanostructure's characteristics. When the working pH in the environment changes from neutral to weakly acidic, the proline amide bonds will undergo *cis–trans* isomerization, which induces the reversible assembly of nanorod-like fibers into nanosphere particles to promote tumor penetration and cellular take up (Fig. 5a).[100]

Light radiation is also a typical stimulus often used in nanomedicine. Wang *et al.* recently prepared a nanomaterial with a transformable shape *via* near-infrared light modulation for long blood circulation and deep tumor penetration *in vivo*. They synthesized a class of nanopolymers based on BF2-azabis (aza-BODIPY) dyes. At a low temperature, dyes are assembled into worm-like nanofibers. With the increase of temperature during light irradiation, the filamentous aggregates in the thermodynamically stable state can transform into spherical-shaped nanoparticles in a metastable aggregation state. With the help of this transformation, more efficient blood circulation and tumor penetration are achieved.[101]

3.2.2 Sphere–rod transformation. Nanoparticles with spherical shapes are most used in nanomedicines, as nanospheres are most easily formed. A series of articles have reported shape conversion from spherical to rod-shaped nanoparticles.[10,102,103] Based on pH-responsive shape-transformable nano-platforms, Han *et al.* prepared a dual-responsive peptide molecule to achieve a shape transformation in response to acidic tumor stimulation. The peptides self-assem-

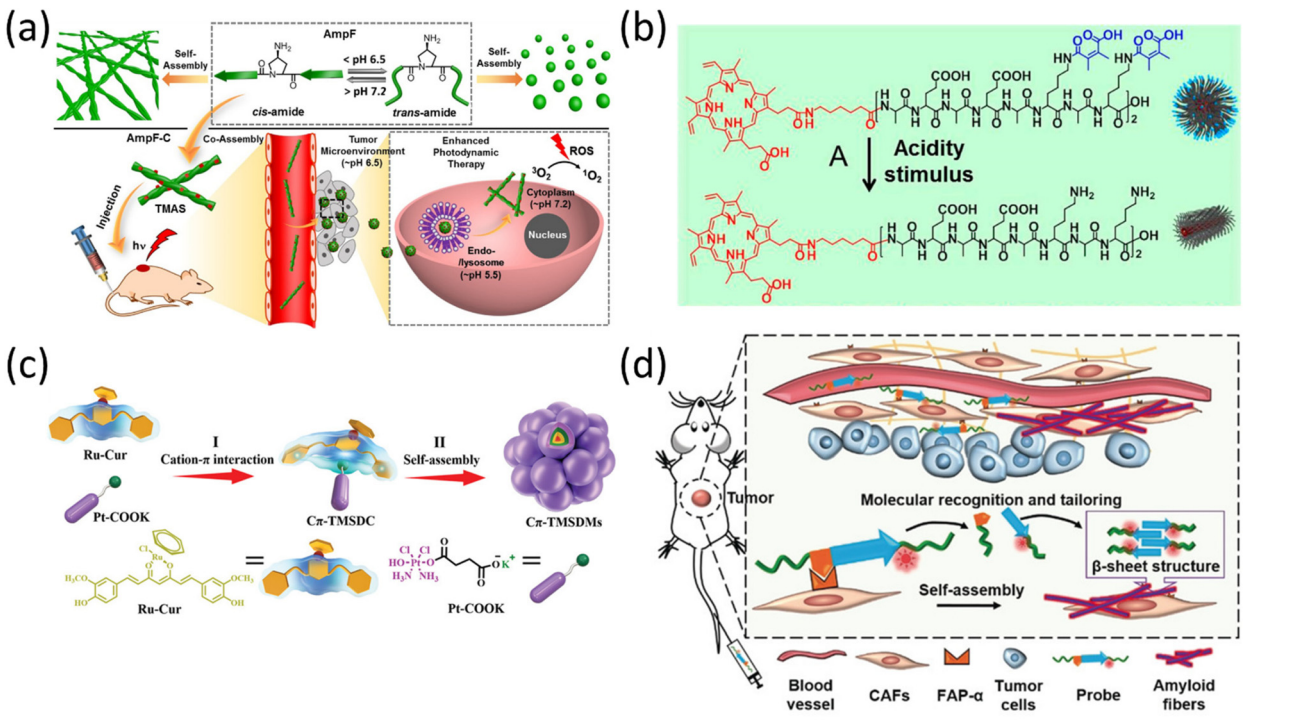

Fig. 5 (a) Creation of nanomedicines capable of prolonging body circulation, facilitating tumor penetration and accumulation, and eventually increasing intracellular retention due to the reversible morphological transition adaptable to the pH gradient present in the cellular take up pathway.[100] Reproduced from ref. 100 with permission from the American Chemical Society, copyright 2019. (b) Mechanism of detachment of DMA under acidity stimulus.[10] Reproduced from ref. 10 with permission from the American Chemical Society, copyright 2017. (c) Formation of the cation–π bridged trimetallic supramolecular drug complex (Cπ-TMSDC) and cation–π-based trimetallic supramolecular drug micelles (Cπ-TMSDMs) in aqueous solution.[102] Reproduced from ref. 102 with permission from Wiley-VCH GmbH, copyright 2022. (d) Schematic illustration of CAF-instructed self-assembly of nanofibers *in situ* for enhanced tumor imaging.[104] Reproduced from ref. 104 with permission from Wiley-VCH GmbH, copyright 2019.

Published on 14 July 2023. Downloaded on 7/11/2024 11:04:51 PM.

ble into nanoparticles with spherical structures, facilitating blood circulation and enrichment in the tumor region through EPR effects. Subsequently, tumor tissue micro-acidity induces the shedding of peptide side chain protecting groups. The rapid transformation of spherical nanoparticles into rod-shaped nanoparticles was driven by hydrogen bonding between peptide molecules and the restoration of hydrophobic forces (Fig. 5b).[10] In this article, rod-shaped nanoparticles significantly enhanced the enrichment of the nanomaterial in tumor tissues. Another example was reported by Liu and colleagues, who also prepared a nanomaterial that achieved acid-realized morphological transformations in the tumor microenvironment for tumor therapy. The drug complex (Cπ-TMSDC) reported in the paper is composed of a cisplatin molecule (Pt-COOK) linked *via* K^+ and another drug with a Ru metal complex containing curcumin (Ru-Cur). Then Cπ-TMSDC further self-assembles into spherical-shaped drug micelles (Cπ-TMSDMs). Due to the strong cation–π interactions, the drug micelles can be stably transported in the blood. However, in the acidic tumor microenvironment, the strong cation–π bond dissociates and promotes the rapid release of rod-shaped Pt-COOK. This transformation enhanced drug permeability while improving therapeutic efficacy (Fig. 5c).[102] Similarly, Kalafatovic *et al.* designed a spherical peptide micelle that was reconfigured to form fibrillar nanostructures after MMP-9-catalyzed hydrolysis.[103]

3.2.3 Other shape transformations. Besides the typical rods and spheres, transformations involving other shapes have also been reported. Peptides and proteins, such as amyloid, self-assembling into fibers and then sheets, can be utilized for designing shape-transforming nanomaterials. Zhao *et al.* designed a shape transition diagnostic system triggered by fibroblast activating protein (FAP-α) for tumor imaging. The probe consists of a short peptide chain, and in the presence of FAP-α, the Gly-Pro-Ala section in the probe molecule is cleaved. The shape transformation is achieved by this cleaving process, which induces proline shedding and the formation of many nanofibers with a β-folded sheet conformation (Fig. 5d).[104] This shape transformation increased the drug retention time and improved the imaging sensitivity. A similar strategy has also been validated for other kinds of enzymes, such as MMPs, PKA and so on, to improve cancer therapy.[105,106]

In another example, Yang *et al.* reported a bispecific supramolecular nanomedicine that achieved a transformable shape in response to GSH for tumor drug delivery. They first synthesized a cyclic peptide in which two flanking cysteine residues formed a cleavable disulfide bond as a reduction trigger. This nanomedicine responds to stimulation by high concentrations of GSH in the tumor. It transforms into a linear peptide when the disulfide bonds in the cyclic peptide structure are broken, which helps to form several hydrogen bonds that can be autonomously assembled into nanofibers.[107] With the help of this transformation, it can suppress tumors well and without serious side effects. Nanomaterials have a variety of morphologies, and through shape-transforming systems and taking advantage of different morphologies simultaneously, nanomaterials have more possible applications.

3.3 Charge transformation

The surface charge of nanoparticles represents another design feature that can be tailored to extend the cycle life and selectively enhance accumulation at specific target sites. Nanoparticles with neutral and negative surface charges have been shown to reduce the adsorption of serum proteins and inhibit charge interactions with macrophage membranes, thereby extending the circulating half-life.[108] On the other hand, positively charged nanoparticles have better internalization capabilities and higher non-specific take up efficiency in most cells, and positively charged particles promote endosomal release through mechanisms such as the 'proton sponge effect'.[109] Therefore, to effectively deliver nanoparticles to tumors, it is desirable that the surface charge of nanoparticles be neutral or slightly negative when administered intravenously but shift to a positive charge when they reach the tumor site. The charge conversion transformation process largely depends on shifts in the chemical structure of the nanocarrier, such as protonation/deprotonation, bond breakage, molecular structure mutations, *etc.*,[110–112] which are triggered by specific internal or external stimuli. This section of the review presents the main types of charge reversal nanoparticles triggered by several stimulation modalities such as pH, tumor redox environment, tumor proteases, light, and heat.

3.3.1 pH-triggered charge transformation. In general, the tumor environment is more acidic (pH 6.5–6.8) than normal tissues (pH 7.15–7.45), while the pH conditions of endo/lysosomes are even lower (pH 4.5–5.0).[113] The design is based on pH-triggered charge reversal in two ways: (i) cleavage of acid-unstable bonds; and (ii) non-covalent electrostatic interactions.

The breakage of surface chemical bonds usually leads to switches in the physicochemical properties of the nanoparticles. Covalent bonds are generally sensitive to acidic environments including hydrazine, imine, amide, oxime bonds, *etc.*[114,115] One typical example is β-carboxylic amide bonds.[116] Liu *et al.* prepared a nanomaterial that achieved a charge shift from negative to positive in response to the tumor micro-acidic environment for the treatment of glioma. They developed a nanoparticle with a three-layer core–shell structure: from inside to outside, an inner polyethyleneimine (PEI) siRNA complex, a negatively charged citric anhydride grafted poly(lysine) (PLL-CA) layer in the middle, and an outer angiopep-2 modified hemoglobin membrane. In the acidic environment of tumor cells, the amide bond in the intermediate PLL-CA layer breaks, exposing the amino side chain (Fig. 6a), which in turn can induce the rupture of the outermost hemoglobin membrane and shift the charge to positive.[117] With the help of this shift, more efficient blood–brain barrier (BBB) penetration and tumor accumulation are achieved.

Recently, Wang *et al.* reported the tumor acidic microenvironment-responsive cleavage and cascade activation of

 This journal is © The Royal Society of Chemistry 2023

Published on 14 July 2023. Downloaded on 7/11/2024 11:04:51 PM.

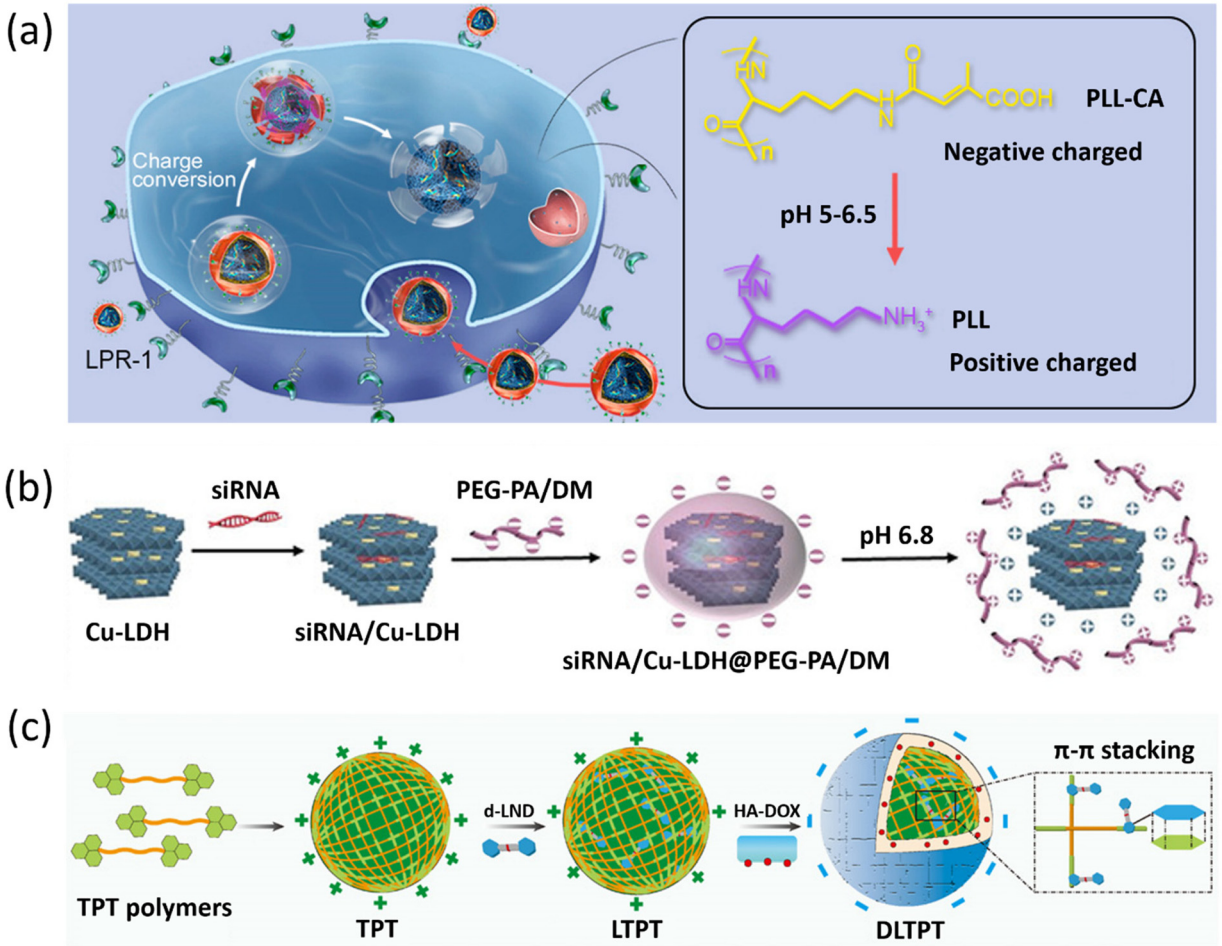

Fig. 6 (a) Mechanism of transformation of charge under acidity stimulus.[117] Reproduced from ref. 117 with permission from the American Chemical Society, copyright 2020. (b) Schematic illustration of the construction, polymer coating and detachment from charge-reversible LDH-based nanoparticles driven by weak acidity.[120] Reproduced from ref. 120 with permission from Wiley-VCH GmbH, copyright 2020. (c) Schematic illustration of the self-assembly process of the cascade-targeting enzyme-sensitive hierarchical nano-platform.[125] Reproduced from ref. 125 with permission from the American Association for the Advancement of Science, copyright 2021.

pendant DMC prodrugs induced by surface charge conversion of nanodrugs from negative to positive for promoting tumor penetration and cellular internalization.[118] Cheng *et al.* have done similar research on the shift of charge from negative to positive. The obtained nanoparticles could maintain a negative charge and have long blood circulation, while undergoing charge reversal at lysosomal pH after endocytosis by cancer cells and boost lysosomal escape.[119]

Compared with acid-labile bond containing systems, non-covalent electrostatic interactions of polymers display a faster response to pH shifts since no breakage of chemical bonds is involved in protonation. Non-covalent electrostatic interactions have been widely utilized to develop core–shell nanostructures by coating cores with negatively charged shells. For example, Liu *et al.* designed acidity-sensitive charge-reversible polymer-coated layered double hydroxide (LDH) nanohybrids. They first synthesized a positively charged LDH and used electrostatic interactions to coat the LDH surface with a negatively charged polymer layer. The nanomaterial has a long circulation time in the blood. In a weakly acidic tumor microenvironment, the negatively charged polymer is hydrolyzed to re-expose the positively charged LDH nanoparticles, achieving a charge shift (Fig. 6b).[120] With the help of this transformation, tumor accumulation and cellular take up functions are performed more efficiently.

3.3.2 Enzyme triggered charge transformation. A number of studies have shown that extracellular proteases regulate switches in many bioactive factors in the tumor microenvironment. Several enzymes are overexpressed in various tumor tissues, such as hyaluronidase (HAase),[121] β-glucuronidase,[122] γ-glutamyl transpeptidase,[123] and esterase.[124] By incorporating specific enzyme substrates into the nanomedicine, these carriers can be recognized and cleaved by the target enzyme. Thus, enzyme-triggered nanomedicines can be designed to achieve on-demand charge transfer by responding to intracellular and extracellular overexpression enzymes. For instance, He *et al.* prepared a nanoparticle that responded to HAase to achieve charge transformation for drug delivery. The

Published on 14 July 2023. Downloaded on 7/11/2024 11:04:51 PM.

team synthesized nanoparticles with a core–shell structure, consisting mainly of a positively charged triphenylphosphonium derivative particle and a negatively charged hyaluronate shell layer. Due to the overexpression of HAase in the tumor microenvironment, the hyaluronic acid shell is degraded by this enzyme upon arrival of the material, thus exposing the positively charged core (Fig. 6c).[125] With the help of this charge transformation, the function of deep penetration into the tumor tissue and effective take up by tumor cells is achieved. In addition, Shen's team recently reported an adhesin that responded to aminopeptidase N and thus achieved tunable charge reversal properties for efficient tumor accumulation and penetration.[126]

In various human tumors, membrane γ-glutamyl transpeptidase (GGT) is overexpressed. GGT cleaves γ-glutamine and has been used for tumor-specific activation of fluorescent probes and drug precursors. For instance, Shen *et al.* developed a GGT-responsive coupling to achieve a shift in charge and thus deliver camptothecin into pancreatic tumor cells. They primarily synthesized a zwitterionic polymer–drug coupling with a long blood circulation time. Once the adjuvant entered the vasculature or tumor mesenchyme, overexpressed GGT hydrolyzed the γ-glutamyl fraction to regenerate the positively charged orthobarbitamine. Subsequently, the positively charged adduct underwent caveolae-mediated endocytosis and transmigration, enabling transendothelial and transcellular transport of the cationic adduct to enhance tumor penetration and anticancer efficacy (Fig. 7a).[127] The team has done similar work using this mechanism, digging deep into nanoparticles' transendothelial route of entering a tumor (Fig. 7b).[128]

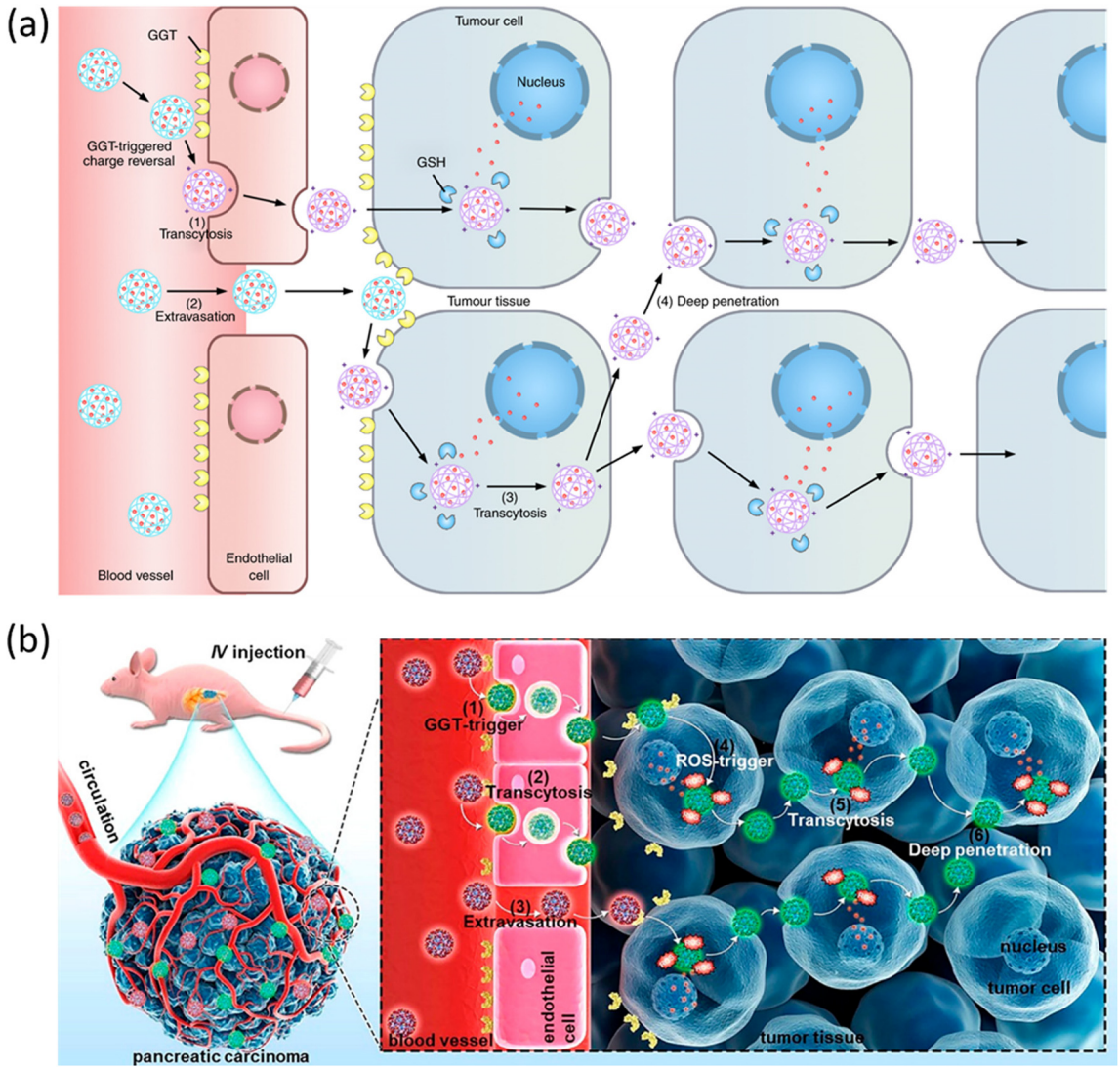

Fig. 7 (a) Illustration of cationization-initiated transcytosis-mediated active tumor penetration for the transendothelial and transcellular transport of the nanomedicine.[127] Reproduced from ref. 127 with permission from Springer Nature, copyright 2019. (b) Illustration of the cationization-initiated transcytosis of GSHPTCPT that bypasses the tPDA tumor ECM, penetrates deep into the tumor, and releases the drug throughout the tumor.[128] Reproduced from ref. 128 with permission from the American Chemical Society, copyright 2020.

This journal is © The Royal Society of Chemistry 2023

Published on 14 July 2023. Downloaded on 7/11/2024 11:04:51 PM.

3.3.3 Other stimuli-responsive charge transformations. In addition to the above-mentioned typical ways to change the nanoparticles' surface charge, other strategies and stimuli have also been reported, such as hypoxia-triggered, ROS-triggered, H_2S-responsive, light-triggered and thermo-responsive, *etc.*[129–132] For example, Shen *et al.* constructed hypoxia-triggered *in situ* auto-loaded fluorescent probes for tumor imaging. They integrated a charge-switchable azobenzene fraction and long-wavelength aggregation-induced emission fluorescence (AIEgens) into a water-soluble polymer. Under tumor hypoxia, the enzymatic reduction of azobenzene triggers the conversion of cationic quaternary ammonium salts into anionic carboxylates, which form nanoparticles after the chain segment polymer undergoes autonomous loading, relying on intermolecular electrostatic interactions.[129] This shift enables the more efficient application of tumor fluorescence imaging. The charge is one of the most critical features of nanoparticles, and research on this issue is ongoing.

3.4 Other physicochemical property transformations

In addition to manipulating the particle size, shape, and surface charge of nanomaterials that can enhance drug delivery efficiency to some extent, many studies have now reported other properties that can also significantly affect the nano–bio interaction, such as the surface roughness, mobility, and mechanical properties of nanomaterials.[133–135] Unfortunately, few articles are related to the preparation of nanomaterials with switching abilities for these properties or such preparations are not yet used for biomedical applications.

3.4.1 Mobility. In recent years, many researchers have invested a lot of effort in the design and construction of self-propelled nanomotors. Due to the excellent ability of nanomotors to have a wide diffusion range, adequate cargo transportation, and deep tissue penetration, nanomotors have good prospects for applications in various fields, such as environmental remediation, cargo transportation, sensing, biomedicine, *etc.*[136–139] Furthermore, in the biomedical field, a large amount of literature reveals that the motility of nanoparticles affects the penetration process of nanoparticles into solid organs and cells.[140–142] Thus tuning of nanomaterials' motion can be of great use. One of the keys to the primary motion of nanoparticles is the ability to apply a continuous asymmetric force on the nanoparticles. In the currently prepared nanomotors, there are two primary sources of this force: mass and energy exchange between the nanoparticle and its surroundings, and that applied directly to the nanoparticle externally.[143,144] Our group introduced a near-infrared "optical brake" into a glucose-driven enzyme-based mesoporous nanomotor to achieve remote speed regulation for the first time. The nanomotor is mainly composed of SiO_2@Au core–shell nanospheres and enzyme-modified periodic mesoporous organosilica (PMO), forming nanoparticles with a Janus mesoporous structure (Fig. 8a).[134] The nanomotor is driven by glucose as a biofuel catalyzed by enzymes (glucose oxidase/hydrogen peroxidase) on the PMO structural domain of this Janus structure, while the Au nanoshell layer in the SiO_2@Au region is capable of generating local thermal gradients under NIR light irradiation to drive the nanomotor by thermoelectrophoresis. Using the unique Janus nanostructure, the driving force generated by enzyme catalysis is in the opposite direction to the thermal conductivity generated by the NIR photothermal effect, thus achieving motion-tunable nanomaterials. Yet still, researchers are no longer satisfied with just making nanoparticles move actively, but are looking forward to achieving the precise control of the motion behaviour of nanomotors. So further studies are needed to determine how such nanomotors can be suitably applied to living organisms and spontaneously respond to various biological barriers.[134]

3.4.2 Surface roughness. As one of the essential parameters of nanocarriers, surface roughness plays a vital role in determining biomolecule binding, phagocytosis, cellular interactions, and biodistribution of nanocarriers.[145–147] By investigating the relevant literature, it was found that a rough surface could enhance the take up of nanocarriers by tumor-associated cells and improve drug delivery efficiency. It may also induce enhanced adhesion of nanocarriers to proteins during the blood circulation phase and promote the take up of nanocarriers by non-target tissues, which is not favorable for targeted drug delivery.[148,149] However, these works only synthesize nanoparticles with different roughness, and more reports are needed on the *in situ* controlled transformation of the roughness of individual particles. Encouragingly, our group recently made some breakthroughs in roughness-transformable nanoparticles. U/DCNP@vSiO_2 (vSiO_2 = viral mesoporous SiO_2) nanoparticles with a rough surface are coated with pH-responsive polymers to "shed" the surface roughness (Fig. 8b).[133] Under normal physiological conditions, this nanocarrier has a smooth polymer surface, weak interactions with proteins/non-target tissues, and prolonged blood circulation time. While in the tumor micro-acidic environment, the polymer shell is detached from the surface, exposing the surface spine-like structure, enhancing its penetration and retention ability in tumor tissues and promoting the take up of the nanocarrier by tumor cells. In addition, molecular dynamics simulations were introduced to simulate the experimental results computationally (Fig. 8c).[133]

3.4.3 Mechanical properties. In recent years, with the improvement of means of characterization, it has been gradually found that the mechanical properties of nanoparticles also play an important role in modulating biological properties.[150–152] Previously in this field, most articles reported on the preparation of nanomaterials with different stiffness, and investigating the need for material softness for different biological barriers. It was found that stiff nanoparticles performed better during blood circulation and tumor accumulation, and deformable nanoparticles were better for penetration, cellular internalization and drug release.[135] Recently, Teng's group reported for the first time a nanoparticle that achieved stiffness deformability in response to GSH and used it to enhance tumor therapeutic effects. They first synthesized manganese oxide-doped mesoporous organosilica nanoparticles with spherical morphology. When they reach high

Published on 14 July 2023. Downloaded on 7/11/2024 11:04:51 PM.

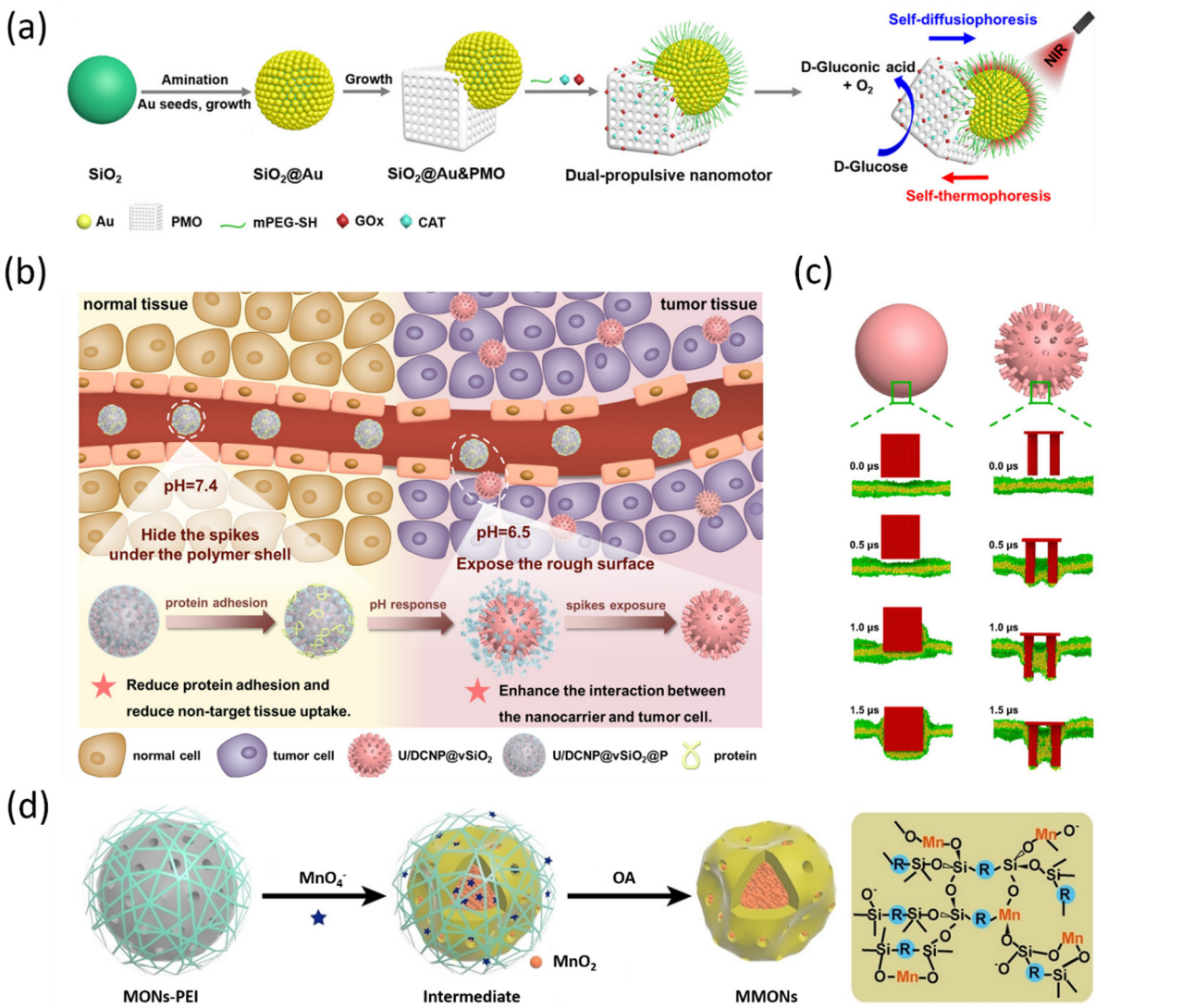

Fig. 8 (a) Schematic illustration of the preparation process and speed regulation mechanism of the dual-propulsive Janus nanomotor.[134] Reproduced from ref. 134 with permission from the American Chemical Society, copyright 2022. (b) Schematic illustration of the tumor microenvironment triggered surface roughness transformable nanocarrier for efficient drug delivery.[133] Reproduced from ref. 133 with permission from Wiley-VCH GmbH, copyright 2023. (c) Simulation of the permeability of smooth and rough surfaces toward the lipid membrane.[133] Reproduced from ref. 133 with permission from Wiley-VCH GmbH, copyright 2023. (d) Schematic illustration of the formation of stiffness-transformable MMONs.[135] Reproduced from ref. 135 with permission from Wiley-VCH GmbH, copyright 2023.

concentrations of GSH in tumor tissues, the Mn–O bonds within the material break, and the rigid nanoparticles are transformed into bowl-shaped nanocapsules (Fig. 8d).[135] The Young's modulus will be reduced from 165.7 MPa to 84.5 MPa. With the unique rigid transformation property of the material, it can better improve the take up of tumor cells and enhance their penetration in the multicellular spheres.

For some physicochemical properties, "transformable" materials have been synthesized, and the nano–bio interactions studied, such as transformation of the mechanical properties of materials, but the synthesized materials are usually macroscale, not nanomaterials.[153] For example, many hydrogels have been prepared with changeable stiffness, and arrays with transformable roughness have also been reported. It would be very desirable if similar approaches could be used for the preparation of nanomaterials with transformable physicochemical properties.

3.5 Dual/multiple physicochemical property transformations

While the transformation of one of a nanomaterial's physicochemical properties may not be enough to tackle all biological barriers, several of these rational design strategies have been combined into single nanoparticle entities in the hope of overcoming as many biological barriers as possible. Our group has recently worked toward developing a platform incorporating several rational design components to overcome biological bar-

 This journal is © The Royal Society of Chemistry 2023

Published on 14 July 2023. Downloaded on 7/11/2024 11:04:51 PM.

riers sequentially. For example, we have designed nanomaterials with dual variable size/charge. Through unstable acid bonding, we immobilized up/downconversion nanoparticles (U/DCNPs) onto large mesoporous silica nanoparticles (MSNs) to form MSN@U/DCNP nano-assemblies with core@satellite structures. Subsequently, the nano-assemblies are encapsulated using charge-reversible polymers (Fig. 9a).[154] At physiological pH, integrated nano-assemblies with a larger size (180 nm) and negative charge can effectively prolong blood circulation and enhance tumor enrichment. In contrast,

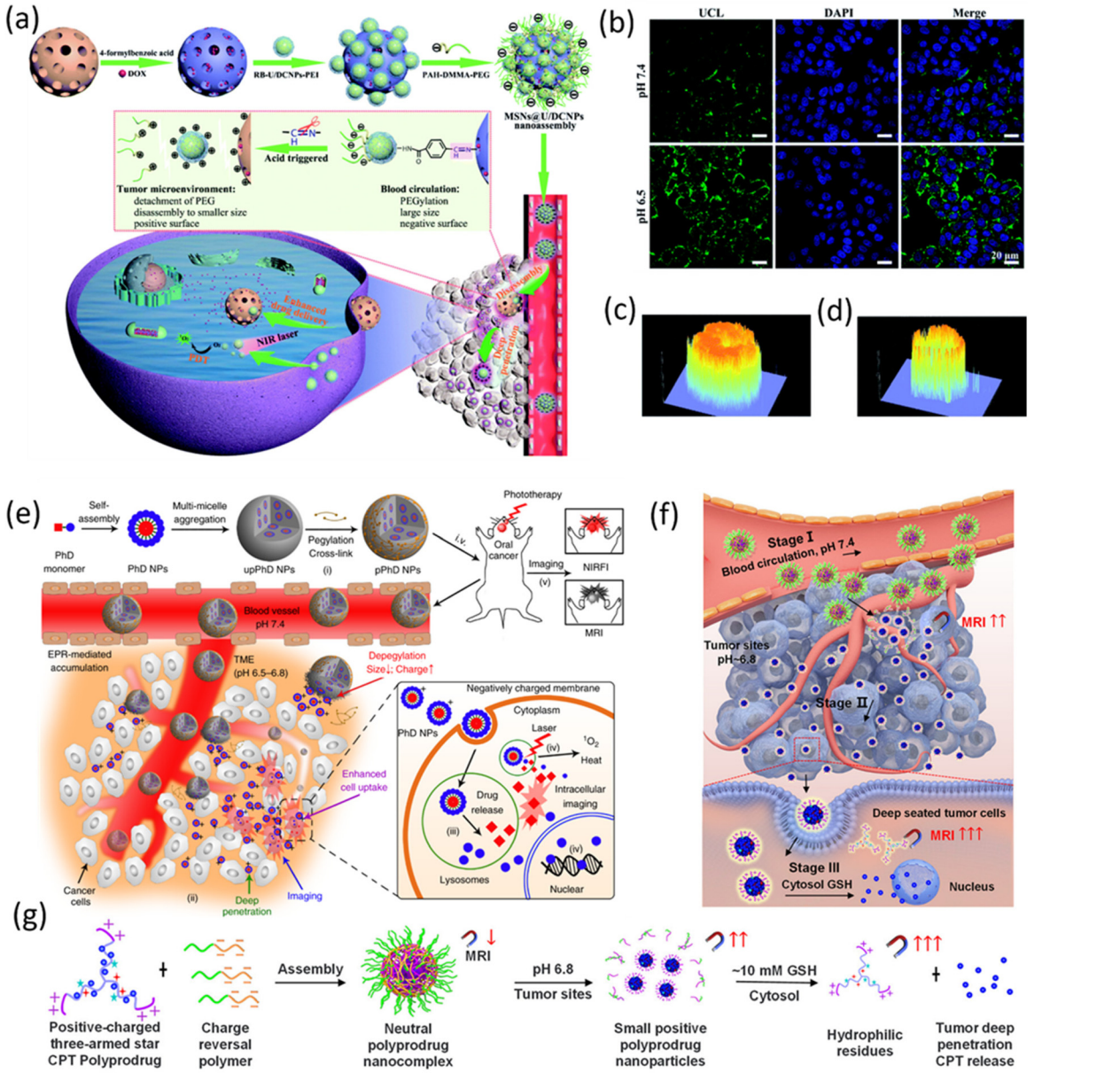

Fig. 9 (a) Schematic illustration of the preparation of core@satellite nanoassemblies and the acidic tumor microenvironment triggered size/charge dual-transformability for combined chemo- and photodynamic therapy (PDT).[154] Reproduced from ref. 154 with permission from the Royal Society of Chemistry, copyright 2020. (b) CLSM images of 4T1 cells treated with MSN@U/DCNPs at pH 6.5 and 7.4.[154] Reproduced from ref. 154 with permission from the Royal Society of Chemistry, copyright 2020. (c and d) 2.5D fluorescence analysis of the CLSM images at a depth of 90 μm.[154] Reproduced from ref. 154 with permission from the Royal Society of Chemistry, copyright 2020. (e) Image illustration of the functionalities of the building blocks and construction of the Trojan horse nanoparticles, and their capability to overcome a series of biological barriers through TME responsiveness, de-PEGylation/crosslinkage, transformability for multimodal imaging and trimodality therapies.[155] Reproduced from ref. 155 with permission from Springer Nature, copyright 2018. (f) Schematic illustration of the formulation of stimuli-responsive polyprodrug nanoparticles (SPNs) with cascade degradation properties, including acid-triggered shell detachment and reduction-responsive parent drug release.[156] Reproduced from ref. 156 with permission from the American Chemical Society, copyright 2020. (g) *In vivo* performance of SPNs for tumor deep-penetration drug delivery monitored by stepwise-enhanced magnetic resonance (MR) signals.[156] Reproduced from ref. 156 with permission from the American Chemical Society, copyright 2020.

Published on 14 July 2023. Downloaded on 7/11/2024 11:04:51 PM.

in an acidic tumor microenvironment, the charge-reversible outer polymer and the connections between MSNs and U/DCNPs break, which induces the splitting of the nanoassemblies into isolated MSNs and smaller U/DCNPs (20 nm) with positively charged surfaces, thus enhancing their take up and permeation effects in tumors and cells (Fig. 9b–d).[154]

Xue *et al.* reported pH-responsive size/charge convertible Trojan horse nanoparticles for delivering ultrasmall, fully active drug adjuvants. They first synthesized an amphiphilic molecule, which linked two adjuvant molecules through hydrazone bonds, and further assembled tiny micelles into relatively large nanocarriers with a size of 79 nm. The reaction with the amino group on the surface of large nanocarriers resulted in the formation of surface Schiff base cross-linked nanoparticles, significantly reducing the positive surface charge. When the ion reaches the acidic environment outside the tumor cells, the surface Schiff base undergoes cleavage, exposing the amino surface with a positive charge and releasing the ultra-small size monomeric particle.[155] The hydrazone bond in adjuvant molecules can be broken in the lysosome, further accelerating drug release. With the help of the dual response transformations, drug penetration and cellular take up in the tumor are greatly facilitated (Fig. 9e). Similarly, Hao *et al.* synthesized stimuli-responsive multidrug nanoparticles (Fig. 9f), which were composed of negatively charged corona and positively charged drug cores (Fig. 9g).[156] In the physiological environment, the nanoparticles can be efficiently accumulated and retained in acidic tumor sites, thus effectively dissociating into positively charged polypeptide nanoparticles with smaller sizes, thus enhancing the intra-tumor penetration and cellular take up effects.[156] Finally, the intracellular CPT parent drug is released in the reducing cytoplasmic environment, thereby activating chemotherapy.

4 Future perspectives

Over the past years, the rational design of nanomedicines was expected to improve anti-tumor efficiency and reduce side effects. As previously discussed, multiple stages are involved in anticancer drug delivery, including circulation in the blood, accumulation in tumor tissues, deep tumor penetration, cellular take up, and drug release within tumor cells. Unfortunately, most conventional nanocarriers could not overcome these barriers, slowing down their clinical translation progress. Therefore, it is widely accepted that more innovation and more efficient nanocarriers represent the future direction of nano-formulation development. In recent years, intelligent transformable nanomedicines, which can transform physicochemical properties in response to endo/exogenous stimuli, have been developed; these are expected to overcome multiple barriers and improve the treatment effect. In this review, we summarized the latest developments in nanomedicines with transformable physicochemical properties, including disassembly and *in situ* assembly of nanomaterials, shape-transformation nanomaterials, charge-reversal nanomaterials, *etc.* Despite rapid progress and the many advantages of intelligent transformable nanomaterials, there are numerous fundamental challenges and opportunities for further application and development.

First, there is still room for improvement in innovation in the design of transformable nanomaterials. Primarily, a series of designs are still based on the physicochemical properties of materials with relatively well-defined mechanisms such as size, charge and shape. For a more systematic and comprehensive understanding of the interaction between the transformable physicochemical properties of nanomaterials and cells, two more aspects can be considered: (i) new methods for controlling the physicochemical properties and new analytical and imaging techniques for a deeper understanding of the microstructure and interactions between nanomaterials and the intra-organismal environment; and (ii) new physicochemical properties of a nanomedicine that can influence the nano–bio interactions, such as surface roughness, mechanical properties, mobility of nanoparticles and so on. There is an urgent need to develop new responsive nanomaterials in this field by exploiting new mechanisms for the construction of nanoparticles. Among the new physicochemical properties mentioned in (ii), the current propulsion mechanism of nanomotors, for example, is relatively simple. Usually, a simple one-step reaction (*e.g.*, catalyzing hydrogen peroxide to produce oxygen, absorbing light to produce heat, *etc.*) generates propulsive forces to drive particle displacement. Unlike synthetic nanomotors, many microorganisms move in a more complex manner. For example, bacteria undergo chemical reactions internally and externally that alter the local internal environment, drive structural changes in specific proteins, and drive flagellar/ciliary oscillatory motions.[157,158] This mechanism enables microbes to perform relatively complex movements. Inspired by the above, the preparation of nanomaterials with advanced nanostructures (*e.g.*, bio-nanostructures) is expected to lead to more efficient and exciting transformation mechanisms.

Second, the response rate of nanomaterials needs to be precisely regulated. Although many current systems are designed for nanomaterials with switchable physicochemical properties, the time span required to change their physicochemical properties is large, ranging from minutes to days, which seriously affects the precise regulation of the interaction between nanomaterials and biological barriers. Therefore, when designing future nanomaterials with switchable physicochemical properties, the relevant response components should be more precisely adjusted so that the response rate can be precisely controlled, enabling further investigation of the effect of physicochemical property switching on the interaction between nanomaterials and biological barriers.

Third, due to the complexity of the environment in living organisms, experimental data and phenomena alone cannot explain the excellent performances of 'smart' materials from a mechanical point of view. With the development of computer technology, and computational simulations of experimental results through molecular dynamics (MD), coarse-grained

 This journal is © The Royal Society of Chemistry 2023

Published on 14 July 2023. Downloaded on 7/11/2024 11:04:51 PM.

molecular dynamics (CGMD), and numerical simulation, it is possible to investigate the process of physicochemical property transformation and to understand the impact of relevant transformations on nano-biological interactions from a microscopic perspective. In general, MD is a microscopic simulation suitable for calculating the reaction and interaction energies between molecules, as well as the hydrophobicity of molecules.[159] In comparison, CGMDs are more suitable for mesoscopic simulations and are often used to model cell membranes, contact angles, and surfactant assembly processes.[160] It is worth mentioning that numerical simulations are more macroscopic analytical techniques and can be used to simulate nanoparticle flow and forces in fluids (*e.g.*, vascular models), diffusion of chemical reactions (*e.g.*, catalysis by Janus nanoparticles), *etc*. Many modules have been developed in COMSOL and MATLAB for numerical simulation calculations.[161]

Fourth, the relationship between nanomaterials with different physicochemical properties and nano-biological interaction interfaces has yet to be studied sufficiently, and thus, advanced imaging and analytical technologies need to be developed. Nano–bio interactions mainly occur in complex biofluids containing large amounts of proteins, nucleic acids, and ions, which can form dynamic corona on the surface of nanomaterials, further changing the overall physicochemical properties of the composite nanomaterials. Due to technical limitations, few types of research have been conducted to directly characterize the changes in elastic modulus/roughness during dynamic interactions. In addition, biological barriers are dynamic systems often disrupted during imaging and characterization, leading to inaccuracies. Therefore, more non-destructive tools and novel *in vivo* facilities are needed to analyze the microstructure and interactions between nanoparticles and the biological environment *in vivo*.

Finally, the biological toxicity of nanomaterials is directly related to their size, surface properties, *etc*. Toxicity studies on nanomaterials with variable physicochemical properties are very complex and require more in-depth studies. The toxicity of nanomaterials before and after switching of the physicochemical properties both need to be taken into account. Factors that stimulate the material to undergo switches, such as light and ultrasound, also require careful study of their effects.

Conflicts of interest

There are no conflicts of interest to declare.

Acknowledgements

The work was supported by the National Natural Science Foundation of China (22075049, 21875043, 22088101, 21701027, 21733003, 21905052, 51961145403), the National Key R&D Program of China (2018YFA0209401), the Fundamental Research Funds for the Central Universities (20720220010), the Key Basic Research Program of the Science and Technology Commission of Shanghai Municipality (22JC1410200), the Natural Science Foundation of Shanghai (22ZR1478900, 18ZR1404600, 20490710600), and the Shanghai Rising-Star Program (20QA1401200, 22YF1402200).

References

1 D. Peer, J. M. Karp, S. Hong, O. C. Farokhzad, R. Margalit and R. Langer, *Nat. Nanotechnol.*, 2007, **2**, 751–760.
2 R. van der Meel, E. Sulheim, Y. Shi, F. Kiessling, W. J. M. Mulder and T. Lammers, *Nat. Nanotechnol.*, 2019, **14**, 1007–1017.
3 M. Bjornmalm, K. J. Thurecht, M. Michael, A. M. Scott and F. Caruso, *ACS Nano*, 2017, **11**, 9594–9613.
4 Y. Dai, C. Xu, X. Sun and X. Chen, *Chem. Soc. Rev.*, 2017, **46**, 3830–3852.
5 Q. Sun, Z. Zhou, N. Qiu and Y. Shen, *Adv. Mater.*, 2017, **29**, 1606628.
6 Q. Sun, X. Sun, X. Ma, Z. Zhou, E. Jin, B. Zhang, Y. Shen, E. A. Van Kirk, W. J. Murdoch, J. R. Lott, T. P. Lodge, M. Radosz and Y. Zhao, *Adv. Mater.*, 2014, **26**, 7615–7621.
7 X. Sun, N. Ni, Y. Ma, Y. Wang and D. T. Leong, *Small*, 2020, **16**, 2003000.
8 L. Zhang, D. Jing, N. Jiang, T. Rojalin, C. M. Baehr, D. Zhang, W. Xiao, Y. Wu, Z. Cong, J. J. Li, Y. Li, L. Wang and K. S. Lam, *Nat. Nanotechnol.*, 2020, **15**, 145–153.
9 S. Ruan, R. Xie, L. Qin, M. Yu, W. Xiao, C. Hu, W. Yu, Z. Qian, L. Ouyang, Q. He and H. Gao, *Nano Lett.*, 2019, **19**, 8318–8332.
10 K. Han, J. Zhang, W. Zhang, S. Wang, L. Xu, C. Zhang, X. Zhang and H. Han, *ACS Nano*, 2017, **11**, 3178–3188.
11 E. Blanco, H. Shen and M. Ferrari, *Nat. Biotechnol.*, 2015, **33**, 941–951.
12 F. Li, Y. Du, J. Liu, H. Sun, J. Wang, R. Li, D. Kim, T. Hyeon and D. Ling, *Adv. Mater.*, 2018, **30**, 1802808.
13 L. Chan, P. Gao, W. Zhou, C. Mei, Y. Huang, X. F. Yu, P. K. Chu and T. Chen, *ACS Nano*, 2018, **12**, 12401–12415.
14 P. P. Yang, Q. Luo, G. B. Qi, Y. J. Gao, B. N. Li, J. P. Zhang, L. Wang and H. Wang, *Adv. Mater.*, 2017, **29**, 1605869.
15 Z. Li, C. Xiao, T. Yong, Z. Li, L. Gan and X. Yang, *Chem. Soc. Rev.*, 2020, **49**, 2273–2290.
16 W. Yu, R. Liu, Y. Zhou and H. Gao, *ACS Cent. Sci.*, 2020, **6**, 100–116.
17 P. Zhang, D. Chen, L. Li and K. Sun, *J. Nanobiotechnol.*, 2022, **20**, 31.
18 H. Chen, Z. Gu, H. An, C. Chen, J. Chen, R. Cui, S. Chen, W. Chen, X. Chen, X. Chen, Z. Chen, B. Ding, Q. Dong, Q. Fan, T. Fu, D. Hou, Q. Jiang, H. Ke, X. Jiang, G. Liu, S. Li, T. Li, Z. Liu, G. Nie, M. Ovais, D. Pang, N. Qiu, Y. Shen, H. Tian, C. Wang, H. Wang, Z. Wang, H. Xu, J.-F. Xu, X. Yang, S. Zhu, X. Zheng, X. Zhang, Y. Zhao, W. Tan, X. Zhang and Y. Zhao, *Sci. China: Chem.*, 2018, **61**, 1503–1552.

Published on 14 July 2023. Downloaded on 7/11/2024 11:04:51 PM.

19 A. S. Mikhail and C. Allen, *J. Controlled Release*, 2009, **138**, 214–223.
20 H. Li, L. Lu, X. Li, P. A. Buffet, M. Dao, G. E. Karniadakis and S. Suresh, *Proc. Natl. Acad. Sci. U. S. A.*, 2018, **115**, 9574–9579.
21 R. Cai and C. Chen, *Adv. Mater.*, 2019, **31**, 1805740.
22 L.-T. Chen and L. Weiss, *Blood*, 1973, **41**, 529–537.
23 X. Li, E. C. Montague, A. Pollinzi, A. Lofts and T. Hoare, *Small*, 2022, **18**, 2104632.
24 B. Wang, X. Su, J. Liang, L. Yang, Q. Hu, X. Shan, J. Wan and Z. Hu, *Mater. Sci. Eng., C*, 2018, **90**, 514–522.
25 M. Petrini, W. J. M. Lokerse, A. Mach, M. Hossann, O. M. Merkel and L. H. Lindner, *Int. J. Nanomed.*, 2021, **16**, 4045–4061.
26 W. Jia, Y. Wang, R. Liu, X. Yu and H. Gao, *Adv. Funct. Mater.*, 2021, **31**, 2009765.
27 J. Shi, P. W. Kantoff, R. Wooster and O. C. Farokhzad, *Nat. Rev. Cancer*, 2017, **17**, 20–37.
28 F. Yuan, M. Dellian, D. Fukumura, M. Leunig, D. Berk, V. Torchilin and R. Jain, *Cancer Res.*, 1995, **55**, 3752–3756.
29 G. Wang, Y. Jiang, J. Xu, J. Shen, T. Lin, J. Chen, W. Fei, Y. Qin, Z. Zhou, Y. Shen and P. Huang, *Adv. Mater.*, 2023, **35**, 2207271.
30 G. Wang, B. Wu, Q. Li, S. Chen, X. Jin, Y. Liu, Z. Zhou, Y. Shen and P. Huang, *Small*, 2020, **16**, 2004172.
31 G. Alexandrakis, E. B. Brown, R. T. Tong, T. D. McKee, R. B. Campbell, Y. Boucher and R. K. Jain, *Nat. Med.*, 2004, **10**, 203–207.
32 M. F. Flessner, J. Choi, K. Credit, R. Deverkadra and K. Henderson, *Clin. Cancer Res.*, 2005, **11**, 3117–3125.
33 C. H. Heldin, K. Rubin, K. Pietras and A. Ostman, *Nat. Rev. Cancer*, 2004, **4**, 806–813.
34 M. Ramachandran, Z. Ma, K. Lin, C. De Souza and Y. Li, *Nanoscale Adv.*, 2022, **4**, 4470–4480.
35 R. Agarwal, V. Singh, P. Jurney, L. Shi, S. V. Sreenivasan and K. Roy, *Proc. Natl. Acad. Sci. U. S. A.*, 2013, **110**, 17247–17252.
36 Y. Hu, S. Gao, A. R. Khan, X. Yang, J. Ji, Y. Xi and G. Zhai, *Expert Opin. Drug Delivery*, 2022, **19**, 221–234.
37 X. Huang, L. Li, T. Liu, N. Hao, H. Liu, D. Chen and F. Tang, *ACS Nano*, 2011, **5**, 5390–5399.
38 T. Yu, A. Malugin and H. Ghandehari, *ACS Nano*, 2011, **5**, 5717–5728.
39 L. Y. Chou, K. Ming and W. C. Chan, *Chem. Soc. Rev.*, 2011, **40**, 233–245.
40 J. Yan, Q. Wu, Z. Zhao, J. Wu, H. Ye, Q. Liang, Z. Zhou, M. Hou, X. Li, Y. Liu and L. Yin, *Biomaterials*, 2020, **255**, 120166.
41 C. He, Y. Hu, L. Yin, C. Tang and C. Yin, *Biomaterials*, 2010, **31**, 3657–3666.
42 M. Zhao, B. Li, P. Wang, L. Lu, Z. Zhang, L. Liu, S. Wang, D. Li, R. Wang and F. Zhang, *Adv. Mater.*, 2018, **30**, 1804982.
43 Y. Wang, S. Li, X. Wang, Q. Chen, Z. He, C. Luo and J. Sun, *Biomaterials*, 2021, **271**, 120737.
44 K. H. Chen, D. J. Lundy, E. K. Toh, C. H. Chen, C. Shih, P. Chen, H. C. Chang, J. J. Lai, P. S. Stayton, A. S. Hoffman and P. C. Hsieh, *Nanoscale*, 2015, **7**, 15863–15872.
45 J. Chen, J. Ding, Y. Wang, J. Cheng, S. Ji, X. Zhuang and X. Chen, *Adv. Mater.*, 2017, **29**, 1701170.
46 H. J. Li, J. Z. Du, X. J. Du, C. F. Xu, C. Y. Sun, H. X. Wang, Z. T. Cao, X. Z. Yang, Y. H. Zhu, S. Nie and J. Wang, *Proc. Natl. Acad. Sci. U. S. A.*, 2016, **113**, 4164–4169.
47 Q. Guo, X. He, C. Li, Y. He, Y. Peng, Y. Zhang, Y. Lu, X. Chen, Y. Zhang, Q. Chen, T. Sun and C. Jiang, *Adv. Sci.*, 2019, **6**, 1901430.
48 P. Ray, L. Alhalhooly, A. Ghosh, Y. Choi, S. Banerjee, S. Mallik, S. Banerjee and M. Quadir, *ACS Biomater. Sci. Eng.*, 2019, **5**, 1354–1365.
49 X. Cun, M. Li, S. Wang, Y. Wang, J. Wang, Z. Lu, R. Yang, X. Tang, Z. Zhang and Q. He, *Nanoscale*, 2018, **10**, 9935–9948.
50 Z. Cong, L. Zhang, S. Q. Ma, K. S. Lam, F. F. Yang and Y. H. Liao, *ACS Nano*, 2020, **14**, 1958–1970.
51 Z. Cao, Y. Ma, C. Sun, Z. Lu, Z. Yao, J. Wang, D. Li, Y. Yuan and X. Yang, *Chem. Mater.*, 2018, **30**, 517–525.
52 X. Ma, X. Chen, Z. Yi, Z. Deng, W. Su, G. Chen, L. Ma, Y. Ran, Q. Tong and X. Li, *ACS Appl. Mater. Interfaces*, 2022, **14**, 26431–26442.
53 T. Zhao, P. Wang, Q. Li, A. A. Al-Khalaf, W. N. Hozzein, F. Zhang, X. Li and D. Zhao, *Angew. Chem., Int. Ed.*, 2018, **57**, 2611–2615.
54 J. Z. Du, H. J. Li and J. Wang, *Acc. Chem. Res.*, 2018, **51**, 2848–2856.
55 J. Z. Du, T. M. Sun, W. J. Song, J. Wu and J. Wang, *Angew. Chem., Int. Ed.*, 2010, **49**, 3621–3626.
56 J. Z. Du, C. Q. Mao, Y. Y. Yuan, X. Z. Yang and J. Wang, *Biotechnol. Adv.*, 2014, **32**, 789–803.
57 J. Liu, X. Guo, Z. Luo, J. Zhang, M. Li and K. Cai, *Nanoscale*, 2018, **10**, 13737–13750.
58 E. H. C. P. Jencks, *J. Am. Chem. Soc.*, 1962, **84**, 832–837.
59 K. Zhou, Y. Wang, X. Huang, K. Luby-Phelps, B. D. Sumer and J. Gao, *Angew. Chem., Int. Ed.*, 2011, **50**, 6109–6114.
60 C. Yuan, K. Raghupathi, B. C. Popere, J. Ventura, L. Dai and S. Thayumanavan, *Chem. Sci.*, 2014, **5**, 229–234.
61 Q. Wang, C. Zou, L. Wang, X. Gao, J. Wu, S. Tan and G. Wu, *Acta Biomater.*, 2019, **94**, 469–481.
62 T. Ma, R. Chen, N. Lv, Y. Chen, H. Qin, H. Jiang and J. Zhu, *Small*, 2022, **18**, 2106291.
63 Y. Guo, Y. Fan, G. Li, Z. Wang, X. Shi and M. Shen, *ACS Appl. Mater. Interfaces*, 2021, **13**, 55815–55826.
64 Q. Pei, X. Hu, X. Zheng, S. Liu, Y. Li, X. Jing and Z. Xie, *ACS Nano*, 2018, **12**, 1630–1641.
65 N. Patel, P. Pera, P. Joshi, M. Dukh, W. A. Tabaczynski, K. E. Siters, M. Kryman, R. R. Cheruku, F. Durrani, J. R. Missert, R. Watson, T. Y. Ohulchanskyy, E. C. Tracy, H. Baumann and R. K. Pandey, *J. Med. Chem.*, 2016, **59**, 9774–9787.
66 S. N. Thomas, A. J. van der Vlies, C. P. O'Neil, S. T. Reddy, S. S. Yu, T. D. Giorgio, M. A. Swartz and J. A. Hubbell, *Biomaterials*, 2011, **32**, 2194–2203.

 This journal is © The Royal Society of Chemistry 2023

Published on 14 July 2023. Downloaded on 7/11/2024 11:04:51 PM.

67 T. Zhang, X. Chen, C. Xiao, X. Zhuang and X. Chen, *Polym. Chem.*, 2017, **8**, 6209–6216.
68 W. Niu, J. Wang, Q. Wang and J. Shen, *Front. Chem.*, 2020, **8**, 574614.
69 W. Fan, W. Bu, B. Shen, Q. He, Z. Cui, Y. Liu, X. Zheng, K. Zhao and J. Shi, *Adv. Mater.*, 2015, **27**, 4155–4161.
70 C. Xu, Y. Yan, J. Tan, D. Yang, X. Jia, L. Wang, Y. Xu, S. Cao and S. Sun, *Adv. Funct. Mater.*, 2019, **29**, 1808146.
71 Z. Fan, B. Jiang, Q. Zhu, S. Xiang, L. Tu, Y. Yang, Q. Zhao, D. Huang, J. Han, G. Su, D. Ge and Z. Hou, *ACS Appl. Mater. Interfaces*, 2020, **12**, 14884–14904.
72 C. Wang, S. Chen, Y. Wang, X. Liu, F. Hu, J. Sun and H. Yuan, *Adv. Mater.*, 2018, **30**, 1706407.
73 Q. Sun, H. Bi, Z. Wang, C. Li, X. Wang, J. Xu, H. Zhu, R. Zhao, F. He, S. Gai and P. Yang, *Biomaterials*, 2019, **223**, 119473.
74 J. Kim, C. Jo, W. G. Lim, S. Jung, Y. M. Lee, J. Lim, H. Lee, J. Lee and W. J. Kim, *Adv. Mater.*, 2018, **30**, 1707557.
75 X. Sun, J. Zhang, C. Yang, Z. Huang, M. Shi, S. Pan, H. Hu, M. Qiao, D. Chen and X. Zhao, *ACS Appl. Mater. Interfaces*, 2019, **11**, 11865–11875.
76 L. Hou, D. Chen, L. Hao, C. Tian, Y. Yan, L. Zhu, H. Zhang, Y. Zhang and Z. Zhang, *Nanoscale*, 2019, **11**, 20030–20044.
77 Y. Niu, J. Zhu, Y. Li, H. Shi, Y. Gong, R. Li, Q. Huo, T. Ma and Y. Liu, *J. Controlled Release*, 2018, **277**, 35–47.
78 L. Mei, J. Rao, Y. Liu, M. Li, Z. Zhang and Q. He, *J. Controlled Release*, 2018, **292**, 67–77.
79 Y. Wang, H. Li, Q. Jin and J. Ji, *Chem. Commun.*, 2016, **52**, 582–585.
80 H. Li, Y. Chen, Z. Li, X. Li, Q. Jin and J. Ji, *Biomacromolecules*, 2018, **19**, 2007–2013.
81 K. Y. Ju, J. Kang, J. Pyo, J. Lim, J. H. Chang and J. K. Lee, *Nanoscale*, 2016, **8**, 14448–14456.
82 X. Ai, C. J. Ho, J. Aw, A. B. Attia, J. Mu, Y. Wang, X. Wang, Y. Wang, X. Liu, H. Chen, M. Gao, X. Chen, E. K. Yeow, G. Liu, M. Olivo and B. Xing, *Nat. Commun.*, 2016, **7**, 10432.
83 S. Ruan, C. Hu, X. Tang, X. Cun, W. Xiao, K. Shi, Q. He and H. Gao, *ACS Nano*, 2016, **10**, 10086–10098.
84 Y. Cheng, J. Dong and X. Li, *Langmuir*, 2018, **34**, 6117–6124.
85 P. K. Kundu, D. Samanta, R. Leizrowice, B. Margulis, H. Zhao, M. Borner, T. Udayabhaskararao, D. Manna and R. Klajn, *Nat. Chem.*, 2015, **7**, 646–652.
86 P. Wang, Y. Fan, L. Lu, L. Liu, L. Fan, M. Zhao, Y. Xie, C. Xu and F. Zhang, *Nat. Commun.*, 2018, **9**, 2898.
87 D. Zhang, G. B. Qi, Y. X. Zhao, S. L. Qiao, C. Yang and H. Wang, *Adv. Mater.*, 2015, **27**, 6125–6130.
88 Y. Yuan, L. Wang, W. Du, Z. Ding, J. Zhang, T. Han, L. An, H. Zhang and G. Liang, *Angew. Chem., Int. Ed.*, 2015, **54**, 9700–9704.
89 V. Bellat, R. Ting, T. L. Southard, L. Vahdat, H. Molina, J. Fernandez, O. Aras, T. Stokol and B. Law, *Adv. Funct. Mater.*, 2018, **28**, 1803969.
90 J. Song, J. Kim, S. Hwang, M. Jeon, S. Jeong, C. Kim and S. Kim, *Chem. Commun.*, 2016, **52**, 8287–8290.
91 X. Liu, Y. Chen, H. Li, N. Huang, Q. Jin, K. Ren and J. Ji, *ACS Nano*, 2013, **7**, 6244–6257.
92 D. Hu, H. Li, B. Wang, Z. Ye, W. Lei, F. Jia, Q. Jin, K. F. Ren and J. Ji, *ACS Nano*, 2017, **11**, 9330–9339.
93 Y. Cheng, J. Dong and X. Li, *Langmuir*, 2018, **34**, 6117–6124.
94 X. Cheng, R. Sun, L. Yin, Z. Chai, H. Shi and M. Gao, *Adv. Mater.*, 2017, **29**, 1604894.
95 S. Kuk, B. I. Lee, J. S. Lee and C. B. Park, *Small*, 2017, **13**, 1603139.
96 J. Xu, L. Xu, C. Wang, R. Yang, Q. Zhuang, X. Han, Z. Dong, W. Zhu, R. Peng and Z. Liu, *ACS Nano*, 2017, **11**, 4463–4474.
97 P. L. Chariou, K. L. Lee, J. K. Pokorski, G. M. Saidel and N. F. Steinmetz, *J. Phys. Chem. B*, 2016, **120**, 6120–6129.
98 T. J. Moyer, J. A. Finbloom, F. Chen, D. J. Toft, V. L. Cryns and S. I. Stupp, *J. Am. Chem. Soc.*, 2014, **136**, 14746–14752.
99 X. X. Li, J. Chen, J. M. Shen, R. Zhuang, S. Q. Zhang, Z. Y. Zhu and J. B. Ma, *Int. J. Pharm.*, 2018, **545**, 274–285.
100 M. Li, Y. Ning, J. Chen, X. Duan, N. Song, D. Ding, X. Su and Z. Yu, *Nano Lett.*, 2019, **19**, 7965–7976.
101 Y. Chen, X. H. Zhang, D. B. Cheng, Y. Zhang, Y. Liu, L. Ji, R. Guo, H. Chen, X. K. Ren, Z. Chen, Z. Y. Qiao and H. Wang, *ACS Nano*, 2020, **14**, 3640–3650.
102 C. Liu, M. Li, J. Sun, P. Li, Y. Bai, J. Zhang, Y. Qian, M. Shi, J. He, H. Huo, J. Pang, L. Fan and W. Tian, *Adv. Funct. Mater.*, 2022, **32**, 2205043.
103 D. Kalafatovic, M. Nobis, J. Son, K. I. Anderson and R. V. Ulijn, *Biomaterials*, 2016, **98**, 192–202.
104 X. X. Zhao, L. L. Li, Y. Zhao, H. W. An, Q. Cai, J. Y. Lang, X. X. Han, B. Peng, Y. Fei, H. Liu, H. Qin, G. Nie and H. Wang, *Angew. Chem., Int. Ed.*, 2019, **58**, 15287–15294.
105 A. Tanaka, Y. Fukuoka, Y. Morimoto, T. Honjo, D. Koda, M. Goto and T. Maruyama, *J. Am. Chem. Soc.*, 2015, **137**, 770–775.
106 M. J. Webber, C. J. Newcomb, R. Bitton and S. I. Stupp, *Soft Matter*, 2011, **7**, 9665–9672.
107 D. S. Yang, Y. H. Yang, Y. Zhou, L. L. Yu, R. H. Wang, B. Di and M. M. Niu, *Adv. Funct. Mater.*, 2020, **30**, 1904969.
108 F. Alexis, E. Pridgen, L. K. Molnar and O. C. Farokhzad, *Mol. Pharm.*, 2008, **5**, 505–515.
109 A. E. Nel, L. Madler, D. Velegol, T. Xia, E. M. Hoek, P. Somasundaran, F. Klaessig, V. Castranova and M. Thompson, *Nat. Mater.*, 2009, **8**, 543–557.
110 F. Cheng, Q. Pan, W. Gao, Y. Pu, K. Luo and B. He, *ACS Appl. Mater. Interfaces*, 2021, **13**, 29257–29268.
111 Z. Chen, L. Wan, Y. Yuan, Y. Kuang, X. Xu, T. Liao, J. Liu, Z. Q. Xu, B. Jiang and C. Li, *ACS Biomater. Sci. Eng.*, 2020, **6**, 3375–3387.
112 Z. Yang, N. Sun, R. Cheng, C. Zhao, Z. Liu, X. Li, J. Liu and Z. Tian, *Biomaterials*, 2017, **147**, 53–67.
113 W. Wu, L. Luo, Y. Wang, Q. Wu, H. B. Dai, J. S. Li, C. Durkan, N. Wang and G. X. Wang, *Theranostics*, 2018, **8**, 3038–3058.
114 Z. Yang, N. Sun, R. Cheng, C. Zhao, Z. Liu, X. Li, J. Liu and Z. Tian, *Biomaterials*, 2017, **147**, 53–67.

Published on 14 July 2023. Downloaded on 7/11/2024 11:04:51 PM.

115 Y. Chang, J. Y. Chen, J. Yang, T. Lin, L. Zeng, J. F. Xu, J. L. Hou and X. Zhang, *ACS Appl. Mater. Interfaces*, 2019, **11**, 38497–38502.
116 H. Kim, S. Kim, S. Kang, Y. Song, S. Shin, S. Lee, M. Kang, S. H. Nam and Y. Lee, *Angew. Chem., Int. Ed.*, 2018, **57**, 12468–12472.
117 Y. Liu, Y. Zou, C. Feng, A. Lee, J. Yin, R. Chung, J. B. Park, H. Rizos, W. Tao, M. Zheng, O. C. Farokhzad and B. Shi, *Nano Lett.*, 2020, **20**, 1637–1646.
118 Y. Wang, Y. Cong, M. Cai, X. Liang, L. Wang and D. Zhou, *J. Controlled Release*, 2023, **356**, 567–579.
119 F. Cheng, Q. Pan, W. Gao, Y. Pu, K. Luo and B. He, *ACS Appl. Mater. Interfaces*, 2022, **14**, 19077.
120 J. Liu, Y. Wu, C. Fu, B. Li, L. Li, R. Zhang, T. Xu and Z. P. Xu, *Small*, 2020, **16**, 2002115.
121 J. X. Tan, X. Y. Wang, H. Y. Li, X. L. Su, L. Wang, L. Ran, K. Zheng and G. S. Ren, *Int. J. Cancer*, 2011, **128**, 1303–1315.
122 B. Sperker, U. Werner, T. E. Murdter, C. Tekkaya, P. Fritz, R. Wacke, U. Adam, M. Gerken, B. Drewelow and H. K. Kroemer, *Naunyn-Schmiedebergs Arch. Pharmacol.*, 2000, **362**, 110–115.
123 E. Obrador, J. Carretero, A. Ortega, I. Medina, V. Rodilla, J. A. Pellicer and J. M. Estrela, *Hepatology*, 2002, **35**, 74–81.
124 R. Niu, H. Jing, Z. Chen, J. Xu, J. Dai and Z. Yan, *Asia-Pac. J. Clin. Oncol.*, 2012, **8**, 362–367.
125 Y. He, L. Lei, J. Cao, X. Yang, S. Cai, F. Tong, D. Huang, H. Mei, K. Luo, H. Gao, B. He and N. A. Peppas, *Sci. Adv.*, 2021, **7**, eaba0776.
126 R. Sun, Y. Zhang, X. Lin, Y. Piao, T. Xie, Y. He, J. Xiang, S. Shao, Q. Zhou, Z. Zhou, J. Tang and Y. Shen, *Angew. Chem., Int. Ed.*, 2023, **62**, e202217408.
127 Q. Zhou, S. Shao, J. Wang, C. Xu, J. Xiang, Y. Piao, Z. Zhou, Q. Yu, J. Tang, X. Liu, Z. Gan, R. Mo, Z. Gu and Y. Shen, *Nat. Nanotechnol.*, 2019, **14**, 799–809.
128 G. Wang, Z. Zhou, Z. Zhao, Q. Li, Y. Wu, S. Yan, Y. Shen and P. Huang, *ACS Nano*, 2020, **14**, 4890–4904.
129 J. Shen, K. Shao, W. Zhang and Y. He, *ACS Macro Lett.*, 2021, **10**, 702–707.
130 X. C. Jiang, J. J. Xiang, H. H. Wu, T. Y. Zhang, D. P. Zhang, Q. H. Xu, X. L. Huang, X. L. Kong, J. H. Sun, Y. L. Hu, K. Li, Y. Tabata, Y. Q. Shen and J. Q. Gao, *Adv. Mater.*, 2019, **31**, 1807591.
131 H. Zhang, X. Kong, Y. Tang and W. Lin, *ACS Appl. Mater. Interfaces*, 2016, **8**, 16227–16239.
132 J. J. Richardson, B. L. Tardy, H. Ejima, J. Guo, J. Cui, K. Liang, G. H. Choi, P. J. Yoo, B. G. De Geest and F. Caruso, *ACS Appl. Mater. Interfaces*, 2016, **8**, 7449–7455.
133 H. Yu, Y. Yu, R. Lin, M. Liu, Q. Zhou, M. Liu, L. Chen, W. Wang, A. A. Elzatahry, D. Zhao and X. Li, *Angew. Chem., Int. Ed.*, 2023, e202216188.
134 M. Liu, L. Chen, Z. Zhao, M. Liu, T. Zhao, Y. Ma, Q. Zhou, Y. S. Ibrahim, A. A. Elzatahry, X. Li and D. Zhao, *J. Am. Chem. Soc.*, 2022, **144**, 3892–3901.
135 J. Tao, Y. Tian, D. Chen, W. Lu, K. Chen, C. Xu, L. Bao, B. Xue, T. Wang, Z. Teng and L. Wang, *Angew. Chem., Int. Ed.*, 2023, e202216361.
136 F. Peng, Y. Tu and D. A. Wilson, *Chem. Soc. Rev.*, 2017, **46**, 5289–5310.
137 P. Diez, E. Lucena-Sanchez, A. Escudero, A. Llopis-Lorente, R. Villalonga and R. Martinez-Manez, *ACS Nano*, 2021, **15**, 4467–4480.
138 D. Dasgupta, D. Pally, D. K. Saini, R. Bhat and A. Ghosh, *Angew. Chem., Int. Ed.*, 2020, **59**, 23690–23696.
139 V. M. Kadiri, C. Bussi, A. W. Holle, K. Son, H. Kwon, G. Schutz, M. G. Gutierrez and P. Fischer, *Adv. Mater.*, 2020, **32**, 2001114.
140 M. Wan, T. Li, H. Chen, C. Mao and J. Shen, *Angew. Chem., Int. Ed.*, 2021, **60**, 13158–13176.
141 Y. Wu, Z. Song, G. Deng, K. Jiang, H. Wang, X. Zhang and H. Han, *Small*, 2021, **17**, e2006877.
142 C. K. Schmidt, M. Medina-Sanchez, R. J. Edmondson and O. G. Schmidt, *Nat. Commun.*, 2020, **11**, 5618.
143 T. Zhao and X. Li, *Adv. Intell. Syst.*, 2023, 2200429.
144 K. Yuan, V. de la Asunción-Nadal, B. Jurado-Sánchez and A. Escarpa, *Chem. Mater.*, 2020, **32**, 1983–1992.
145 Y. Niu, M. Yu, S. B. Hartono, J. Yang, H. Xu, H. Zhang, J. Zhang, J. Zou, A. Dexter, W. Gu and C. Yu, *Adv. Mater.*, 2013, **25**, 6233–6237.
146 M. Li, Z. Liang, C. Chen, G. Yu, Z. Yao, Y. Guo, L. Zhang, H. Bao, D. Fu, X. Yang, H. Wang, C. Xue and B. Sun, *ACS Nano*, 2022, **16**, 10482–10495.
147 P. M. Chen, W. Y. Pan, P. K. Luo, H. N. Phung, Y. M. Liu, M. C. Chiang, W. A. Chang, T. L. Tien, C. Y. Huang, W. W. Wu, W. T. Chia and H. W. Sung, *ACS Nano*, 2021, **15**, 7596–7607.
148 W. Wang, P. Wang, L. Chen, M. Zhao, C.-T. Hung, C. Yu, A. A. Al-Khalaf, W. N. Hozzein, F. Zhang, X. Li and D. Zhao, *Chem*, 2020, **6**, 1097–1112.
149 X. Fan, X. Wu, F. Yang, L. Wang, K. Ludwig, L. Ma, A. Trampuz, C. Cheng and R. Haag, *Angew. Chem., Int. Ed.*, 2022, **61**, e202113833.
150 Y. Chen, X. Li, M. Wang, L. Peng, Z. Yu, X. Peng, J. Song and J. Qu, *Small*, 2020, 1906028.
151 D. Nie, C. Liu, M. Yu, X. Jiang, N. Wang and Y. Gan, *Biomaterials*, 2022, **291**, 121879.
152 X. Peng, K. Chen, W. Liu, X. Cao, M. Wang, J. Tao, Y. Tian, L. Bao, G. Lu and Z. Teng, *Nano-Micro Lett.*, 2020, **12**, 137.
153 C. Zhang, X. Xiao, Y. Zhang, Z. Liu, X. Xiao, A. Nashalian, X. Wang, M. Cao, X. He, J. Chen, L. Jiang and C. Yu, *ACS Nano*, 2022, **16**, 9348–9358.
154 L. Chen, T. Zhao, M. Zhao, W. Wang, C. Sun, L. Liu, Q. Li, F. Zhang, D. Zhao and X. Li, *Chem. Sci.*, 2020, **11**, 2819–2827.
155 X. Xue, Y. Huang, R. Bo, B. Jia, H. Wu, Y. Yuan, Z. Wang, Z. Ma, D. Jing, X. Xu, W. Yu, T. Y. Lin and Y. Li, *Nat. Commun.*, 2018, **9**, 3653.
156 Q. Hao, Z. Wang, W. Zhao, L. Wen, W. Wang, S. Lu, D. Xing, M. Zhan and X. Hu, *ACS Appl. Mater. Interfaces*, 2020, **12**, 49489–49501.
157 M. Kang, M. Seong, D. Lee, S. M. Kang, M. K. Kwak and H. E. Jeong, *Adv. Mater.*, 2022, **34**, 2200185.

 This journal is © The Royal Society of Chemistry 2023

158 S. Li, M. M. Lerch, J. T. Waters, B. Deng, R. S. Martens, Y. Yao, D. Y. Kim, K. Bertoldi, A. Grinthal, A. C. Balazs and J. Aizenberg, *Nature*, 2022, **605**, 76–83.
159 L. Ou, Y. Luo and G. Wei, *J. Phys. Chem. B*, 2011, **115**, 9813–9822.
160 J. Sun, L. Zhang, J. Wang, Q. Feng, D. Liu, Q. Yin, D. Xu, Y. Wei, B. Ding, X. Shi and X. Jiang, *Adv. Mater.*, 2015, **27**, 1402–1407.
161 X. Yi, X. Shi and H. Gao, *Phys. Rev. Lett.*, 2011, **107**, 098101.

Published on 14 July 2023. Downloaded on 7/11/2024 11:04:51 PM.